

1

AD-A170 669

REPORT DOCUMENTATION PAGE		READ INSTRUCTIONS BEFORE COMPLETING FORM
1. REPORT NUMBER AFIT/CI/NR 86- 86T	2. GOVT ACCESSION NO.	3. RECIPIENT'S CATALOG NUMBER
4. TITLE (and Subtitle) Implementation of the Numerical Electromagnetic Code (NEC-2) for Modeling the VOR Navigation System in the Presence of Parasitic Scatterers		5. TYPE OF REPORT & PERIOD COVERED THESIS/Dissertation
		6. PERFORMING ORG. REPORT NUMBER
7. AUTHOR(s) Paul R. Barré		8. CONTRACT OR GRANT NUMBER(s)
9. PERFORMING ORGANIZATION NAME AND ADDRESS AFIT STUDENT AT: Ohio University		10. PROGRAM ELEMENT, PROJECT, TASK AREA & WORK UNIT NUMBERS
11. CONTROLLING OFFICE NAME AND ADDRESS AFIT/NR WPAFB OH 45433-6583		12. REPORT DATE 1986
14. MONITORING AGENCY NAME & ADDRESS (if different from Controlling Office)		13. NUMBER OF PAGES 107
		15. SECURITY CLASS. (of this report) UNCLAS
		15a. DECLASSIFICATION/DOWNGRADING SCHEDULE
16. DISTRIBUTION STATEMENT (of this Report) APPROVED FOR PUBLIC RELEASE; DISTRIBUTION UNLIMITED		
17. DISTRIBUTION STATEMENT (of the abstract entered in Block 20, if different from Report)		
18. SUPPLEMENTARY NOTES APPROVED FOR PUBLIC RELEASE: IAW AFR 190-1		<p><b>SDTC ELECTED</b></p> <p>AUG 12 1986</p> <p><b>D</b></p> <p><i>Lynn E. Wolaver</i></p> <p>LYNN E. WOLAVER 6 AUG 86 Dean for Research and Professional Development AFIT/NR</p>
19. KEY WORDS (Continue on reverse side if necessary and identify by block number)		
20. ABSTRACT (Continue on reverse side if necessary and identify by block number) ATTACHED.		

DTIC FILE COPY

IMPLEMENTATION OF THE NUMERICAL ELECTROMAGNETIC  
CODE (NEC-2) FOR MODELING THE VOR NAVIGATION SYSTEM  
IN THE PRESENCE OF PARASITIC SCATTERERS

A Thesis Presented to  
The Faculty of the College of Engineering and Technology  
Ohio University

In Partial Fulfillment  
of the Requirements for the Degree  
Master of Science

by  
Paul R. Barré  
June 13, 1986

Accession For	
NTIS GRA&I	<input checked="" type="checkbox"/>
DTIC TAB	<input type="checkbox"/>
Unannounced	<input type="checkbox"/>
Justification	
By _____	
Distribution/	
Availability Codes	
Dist	Avail and/or Special
A-1	



## TABLE OF CONTENTS

	<u>Page</u>
I. Introduction and Summary	1
II. Model Development	4
A. The VOR Navigation System -- an Introduction	4
1. The Omnirange Principle	4
2. VOR Basics	6
3. Summarization of VOR Basics	9
B. Theory of Operation for the "Basic VOR Model" (program KCVOR -- Scatterers not simulated)	10
1. VOR System and Signal Construction	13
2. Further Signal Construction and Sampling	15
3. Signal Processing	17
4. Error Determination and output	19
C. Theory of Operation for the "General VOR Model" (program GVOR -- Scatterer simulation possible)	21
1. NEC-2 -- Part One of the "General VOR Model"	22
a. The Numerical Electromagnetics Code (NEC-2)	22
b. An Overview on Modeling Conducting Structures	25
c. Modeling VOR Components Using NEC-2	26
(1) The Alford Loop Antenna	26
(2) The VOR Counterpoise	37
d. The VOR Modulation Scheme	38
e. Description of the NEC-2 Output File	39
2. Program GVOR -- Part Two of the "General VOR Model"	43
a. The NTG (NEC To GVOR) Subroutine	45
b. Processing the NEC-2 Data	46
III. Results	50
A. Model KCVOR	50
B. Model GVOR	52
1. Baseline model output (no scatterer) -- a comparison with KCVOR	52
2. Modeled results of horizontally polarized parasitic scatterers and a comparison to measured data	53

TABLE OF CONTENTS (continued)

	<u>Page</u>
3. Modeled results of vertically polarized parasitic scatterers	65
IV. Recommendations	66
V. Acknowledgements	71
VI. References	72
VII. Appendices	75
A. Algorithm for Calculating the Received Time-Domain VOR Signal	75
B. Code listings	83
1. KCVOR	84
2. KCVOR-M	87
3. GVOR	90
4. NECIN.DAT	95
5. NECSCIN.DAT	97
C. User's Section	100
VIII. Abstract	106

## I. INTRODUCTION AND SUMMARY

This project was funded by the Federal Aviation Administration (FAA) under Contract DTFA01-85-Y-01020. The FAA is interested in collocating VHF communication antennas on VOR sites, rather than obtaining new sites for these antennas. Since, the communication antennas are vertically polarized (the VOR is a horizontally polarized system), it is felt that the chance of success in collocating these antennas on a VOR site without unacceptably degrading the VOR is good. If this proves to be the case, these antennas will be collocated at VOR sites, thus offering considerable cost savings. To physically measure the best place to locate each VHF antenna that is to be put on a VOR site would be prohibitively expensive. For this reason the FAA is interested in the development of a computer model that can predict the optimum placement of VHF communication antennas on a VOR site.

Consequently, a computer model has been developed that estimates bearing error for a VOR airborne navigation system operating in the presence of small, parasitic scatterers such as antennas, antenna masts, and guy wires. Parasitic scatterers are radiating elements whose radiation is induced by other electromagnetic radiation rather than by a connected power source. These parasitic scatterers can disturb the very signals that caused them to radiate. Because this VOR model can account for the effects of an arbitrary parasitic scatterer on VOR performance, it is thought of as a general VOR model and, so, was named GVOR.

Model GVOR uses the Numerical Electromagnetics Code (NEC-2) to model the four Alford Loop antennas in a VOR array, to define small parasitic scatterers, as well as to calculate the effects of these scatterers on the radiation patterns of the four antennas. NEC-2 is a user-oriented computer code for analysis of the electromagnetic response of antennas and other metal structures [1]. This commonly used code has been validated by numerous studies [2], [3], [4], [5]. Because NEC-2 is an established and validated code, it was not modified in the development of the VOR model, so as to preserve its integrity.

Program GVOR, a FORTRAN-77 routine, reads the output from NEC-2 to obtain the pertinent scattered-field data. These data are then used to construct the VOR audio waveform and to calculate the indicated bearing at the airborne receiver location, including the effects of parasitic scattering as given by NEC-2. The azimuth angle of an aircraft with respect to a VOR station is determined by the phase of the received audio sinusoid generated by a limaçon radiation pattern that rotates in space due to appropriate time-varying phasing between four Alford loop antennas. To model the effects of scatterers on system accuracy, each loop antenna is sequentially modeled in the presence of the scatterer using NEC-2, and field data are recorded for a far-field orbit around the source-scatterer configuration; this process is repeated for each of the four loop antennas thus providing complete information about complex path loss between each loop antenna and the observation point in the presence of the scatterer. The received audio waveform is then constructed at each observation point by applying the appropriate

modulation to each of the loop antennas, adjusted by the complex loss values given by NEC-2. Next, the phase and distortion of the received audio waveform is then determined using a Fast Fourier Transform algorithm, giving an indication of VOR degradation due to parasitic scattering. Modeled results, consisting of plots of bearing error versus "true" bearing, are then compared to measured data.

The measured VOR bearing data, which was collected in a previous study [6], is suspected to have problems, however. In some cases the agreement theoretically expected between data from the near zone and data from the far zone is not reflected in the actual measurements. When the modeled data are compared to these cases, the correlation between the modeled and the measured data is not good. However, when the near zone data and the far zone data match up well, so do the modeled data. Although there are suspicions that some of the measured data are bad, the respective comparisons with modeled data were included for completeness. Overall, because the modeled data shows the same periodicity as the measured data, and exhibits nearly the same peak error when the near and far measured data agree, and because of the model's proper prediction of VOR system response (octantal error), it is felt that the modeling approach is valid.

## II. MODEL DEVELOPMENT

### A. Theory of Operation for the VOR Navigation System

#### 1. The Omirange Principle

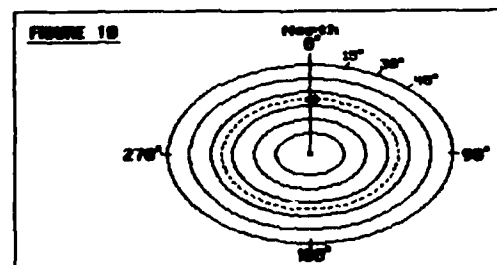
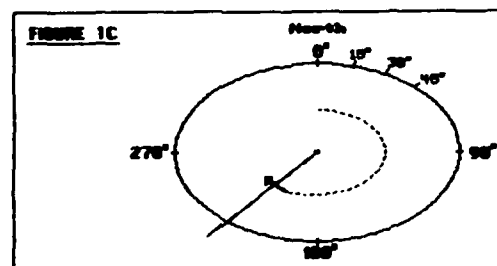
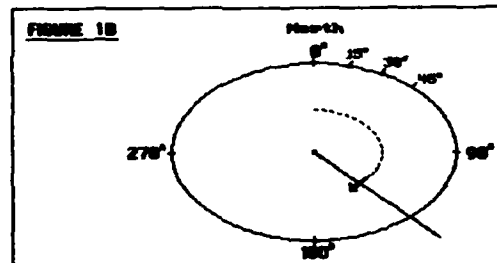
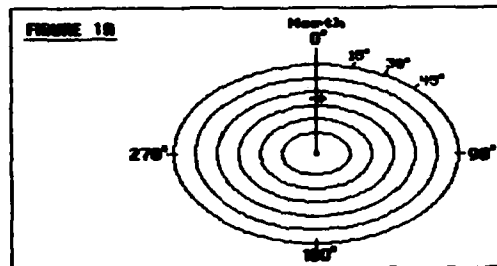
VOR is an acronym for Very-high-frequency Omni-directional Range. This navigational aid, as the name implies, operates in the VHF band of the radio wave spectrum, and radiates its navigation signals in all directions [7]. In understanding the omni-directional range principle (also called "omirange") that is employed by the VOR, the following analogy may be helpful.

Imagine a visible laser beam arranged so that it rotates in a horizontal plane (X-Y for simplicity) at the constant angular frequency of 30 revolutions/sec. Also, imagine an isotropic point source that emits visible light in all directions in observable, yet almost instantaneous, flashes. This point source is collocated with the laser and flashes 30 times per second. The system is synchronized so that the point source flashes when the laser is beaming up the positive Y axis, where the Y axis represents a zero degree radial pointing towards magnetic north. Figures 1A, 1B, 1C, and 1D picturize this hypothetical omirange system. The origin of the circular coordinate system represents the point where the laser and the isotropic source are collocated. The numbers marked with the degree symbol indicate a few of the many possible course bearings (radials). The line extending radially outward from the origin represents the laser beam. In Figure 1A, the laser is rotating clockwise at its constant angular frequency of 30 revolutions/sec, and



is pictured as pointing north, at the zero degree radial. The concentric circles represent the emissions of the synchronized isotropic point source. In Figures 1B and 1C, the laser continues to rotate clockwise, but the point source does not transmit again until the laser is pointing north, as in Figure 1D.

### OMNIRANGE SYSTEM



If an interested observer notes the time when the point source flashes ( $t_1$ ), and also notes the time when the laser points in his or her direction ( $t_2$ ), the observer can deduce radial position with respect to the system in the following manner:

$$(t_2 - t_1)[\text{sec}] * (2 * \text{PI} * 30)[\text{rad/sec}] * (180 / \text{PI})[\text{deg/rad}] = \text{Radial Position}$$

or

$$\text{Radial Position [deg]} = (t_2 - t_1) * 60 * 180$$

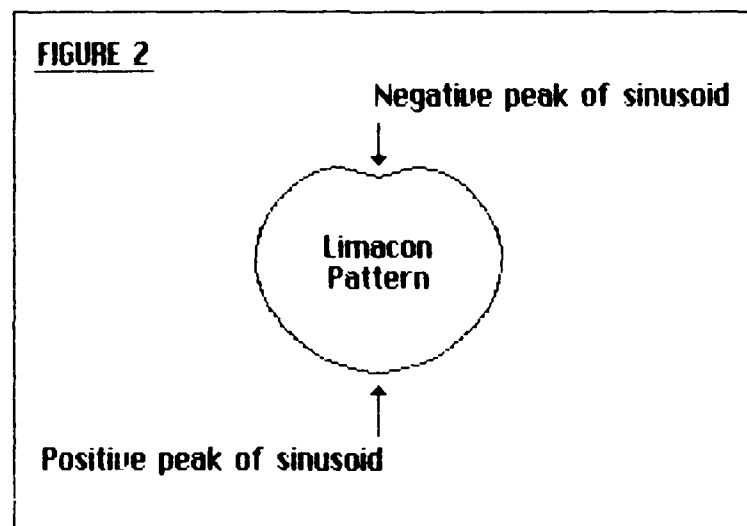
The VOR system uses the omnirange principle in a manner similar to the "point-source & laser" system described above. In the discussion that follows, the *VOR reference signal* is analogous to the isotropic point source, and the *VOR variable signal* is analogous to the laser beam.

## 2. VOR Basics

The following description is that of an ideal VOR system. The VOR navigation system operates in the high frequency band of the RF spectrum with a carrier frequency ranging from 108 to 118 MHz. The navigational information radiated by the VOR is contained in two mutually exclusive, horizontally polarized, 30 Hz signals. To avoid interaction by the two signals, thereby preserving the navigation information, one is frequency modulated upon the carrier (the reference signal), and the other is amplitude modulated upon the carrier (the variable signal). The navigational information is obtained by comparing the relative phases of the two received, demodulated, 30 Hz signals [8].

The *VOR variable signal* is generated by an antenna array that is configured to provide a radiation pattern that has the shape of a

"limaçon" and which rotates at 30 revolutions per second. A limaçon is very similar in appearance to a cardioid but has one main difference: the curvature of a limaçon is sinusoidal. That is, the distance from the center of the limaçon to its border varies sinusoidally as the limaçon is traced out. When a rotating limaçon radiation pattern is observed by a stationary observer, the demodulated variable signal appears sinusoidal, with the frequency of the sinusoid equal to the rate of the limaçon's rotation. Figure 2 shows, for two points on the limaçon, which part of a sinusoid the observer sees when the respective point on the limaçon passes by. This radiated limaçon is the "heart" of the VOR variable signal since the variable signal is actually the limaçon pattern amplitude modulated upon the VHF carrier signal [9].



The main characteristic of the VOR variable signal is that its phase as received by the observer depends upon the radial position of the observer with respect to the VOR. This is a direct result of the rotating limaçon radiation pattern. Another result is that, with the

distance from the VOR held constant, the observed phase of the variable signal changes degree for degree with each change in the radial position (azimuth angle) of the observer around the VOR. The *VOR reference signal*, to the contrary, has the characteristic that its audio phase is independent of the azimuth angle (the radial position of the observer with respect to the VOR). This means that, given a radial distance from the VOR, the phase observed at that distance is constant, independent of the azimuth angle [10].

As mentioned earlier, the navigation information of the VOR is contained in the reference and variable signals. By definition and design, *the angular course about the VOR is equal to the number of degrees by which the variable signal lags the reference signal* [11]. If the VOR is observed at the particular radial of 0 degrees (magnetic north), it would be found that the reference and the variable signals are in phase, similar to the point source flashing when the laser pointed north in the above analogy. If the VOR is then observed from the 5 degree radial, the reference signal would still have the same phase that it did at zero degrees since its phase is independent of azimuth angle, but the variable signal would be delayed 5 degrees from its previously observed phase. Therefore, a course bearing of 5 degrees would be obtained [12].

Theoretically, the VOR can provide an infinite number of courses (radials) to the aircraft because there are an infinite number of radials extending from the VOR. Realistically, the tolerance of the VOR is such that it can accurately provide at least 360 courses, which conveniently converts to one course for each degree of azimuth.

Therefore, VOR instruments in aircraft are calibrated for the 360 degrees of azimuth, with 0 degrees indicating magnetic north. Since the locations of VOR sites are accurately known, an aircraft's position can be established by use of a VOR signal in conjunction with distance measuring equipment (DME), so as to determine not only at what angle the aircraft is from the VOR but also how far away it is. Another method to determine an aircraft's location is to receive bearing data from two nearby VOR'S and then use triangulation for a position fix. VOR's have a range of at least 40 miles and up to about 100 miles [13].

### 3. Summarization of VOR Basics

- \* For a given observation point, both of the received 30 Hz signals, reference and variable, are sinusoids. At 0 degrees azimuth (magnetic north), these two sinusoids are in phase.
- \* The VOR variable signal is so named because its phase varies with respect to the radial position of the observer. The phase of the reference signal, in contrast, remains constant with respect to the radial position of the observer.
- \* The angular course about the VOR is equal to the number of degrees by which the variable signal lags the reference signal.

## B. Theory of Operation for the "Ideal VOR Model" (program KCVOR)

Initial work with VOR modeling was directed at characterizing the performance of an ideal system, one that was not influenced by parasitic scattering. This initial work resulted in a model named KCVOR, which was shown to be operating properly by its correct estimation of octantal errors and system response to variations in the Alford Loop antenna patterns. The VOR model that does account for parasitic scattering effects, BVOR, is an extension of KCVOR, and thus an understanding of the theory of operation of KCVOR is a necessary background for the understanding of BVOR.

KCVOR was designed to estimate VOR bearing error for the following scenario: An airplane flies a circular orbit around a VOR facility at a pre-determined elevation and radius. For equi-spaced observation points around the orbit ( $5^\circ$  azimuth angle increments), one period of the VOR's signal ( $1/30$  of a second) is sampled. This is done 73 times, once for every  $5^\circ$  between  $0^\circ$  and  $360^\circ$ , inclusive. But before the next sample is taken, the present sample is analyzed for its navigation information. That is, a radial measurement is obtained from the sample that tells how many degrees in azimuth the aircraft is from magnetic north of the VOR facility. This derived position is then compared to the true azimuthal position of the aircraft, which is defined explicitly by the model. The modeled VOR bearing error, which is the difference between the two position values, is saved at each azimuth angle sampled. At the end of the modeled flight, an error curve is generated using the saved values. The different errors obtained around the orbit are displayed versus the

true radial position of the aircraft, thereby giving a graphical indication of how well the modeled VOR performed.

Many VOR system parameters can be varied within KCVOR. This includes the system's carrier frequency, the Alford Loop antenna positions and radiation patterns, the phase shift and/or attenuation in any of the four Alford Loop antennas, and the modulation scheme produced by the goniometer (the VOR variable signal generator).

A flowchart of KCVOR is illustrated in Figure 3. It should be noted that no mention is made of the VOR reference signal in this algorithm. Recall that one of the characteristics of the VOR reference signal is that its phase is constant at a given radial distance from the VOR, independent of the azimuth angle. The model uses this property rather than constructing the reference signal in the program. Because time and source/observer geometry are calculated by the model, the audio phase of the reference signal can be computed at any point in space. The only assumption made in the model estimation of the reference signal is that the audio phase of that signal is not affected by multipath effects, a reasonable assumption for the modulation and carrier frequencies involved. In the model, the reference and variable signal audio phases are equal at zero degrees azimuth, as is true with an actual VOR installation. The bearing angle, as determined by the VOR, is the audio phase angle difference between the reference and variable signal.

### FLOWCHART OF KCUOR

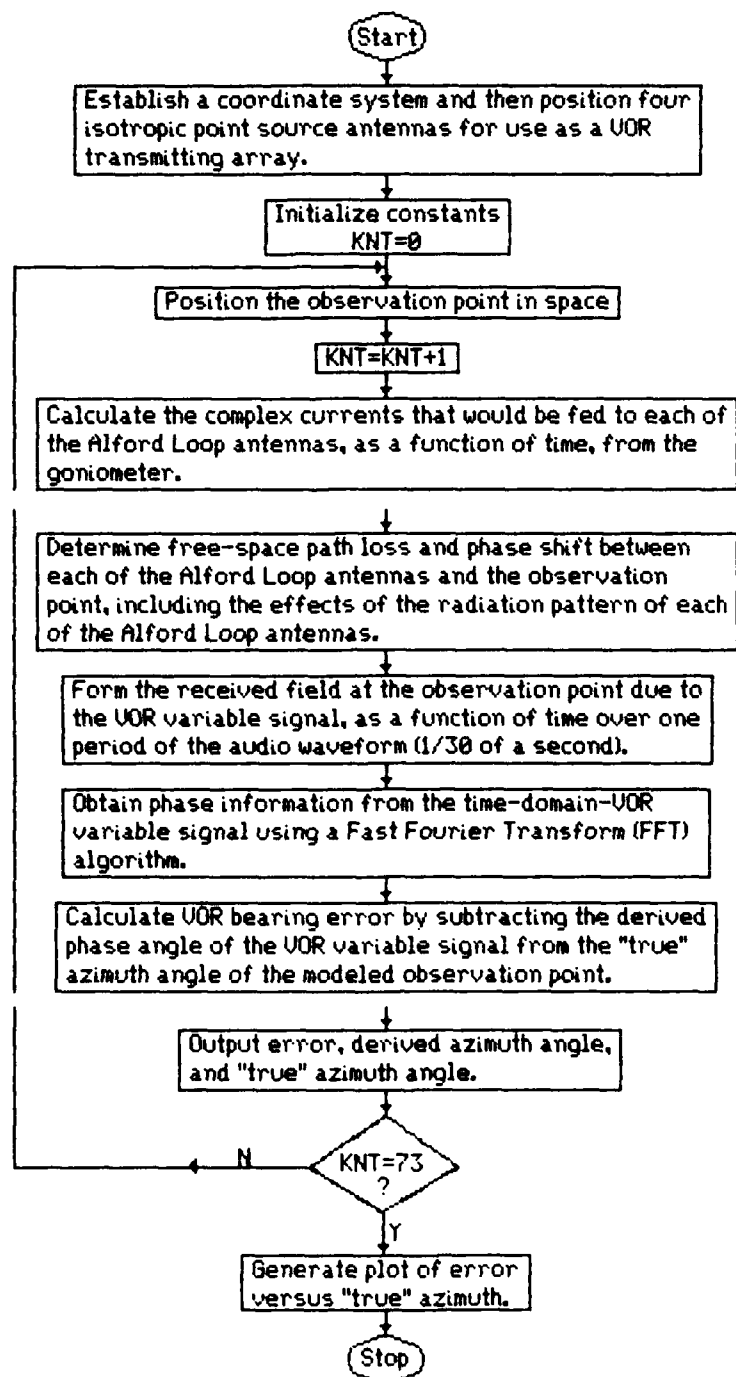


**Figure 3:** Flowchart of ideal UOR model -- program KCUOR



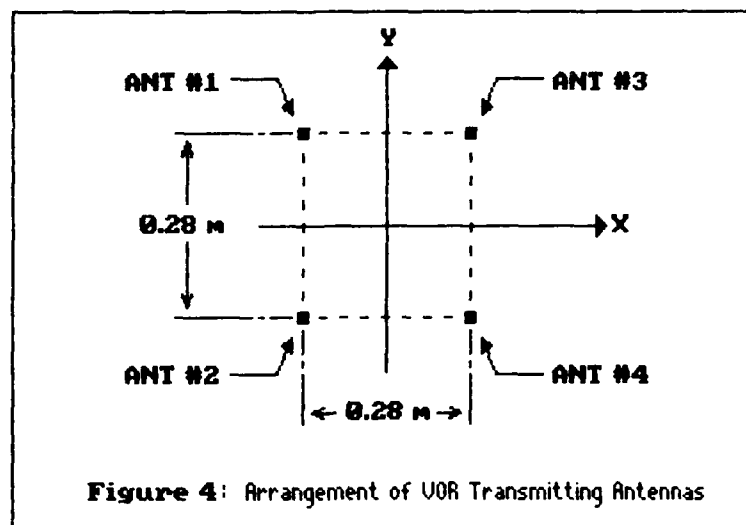
Model operation, as described in the flowchart, can be broken down into four distinct categories:

- \* system construction and initialization
- \* signal construction and sampling
- \* signal processing
- \* bearing error determination and output.

#### 1) System construction and initialization

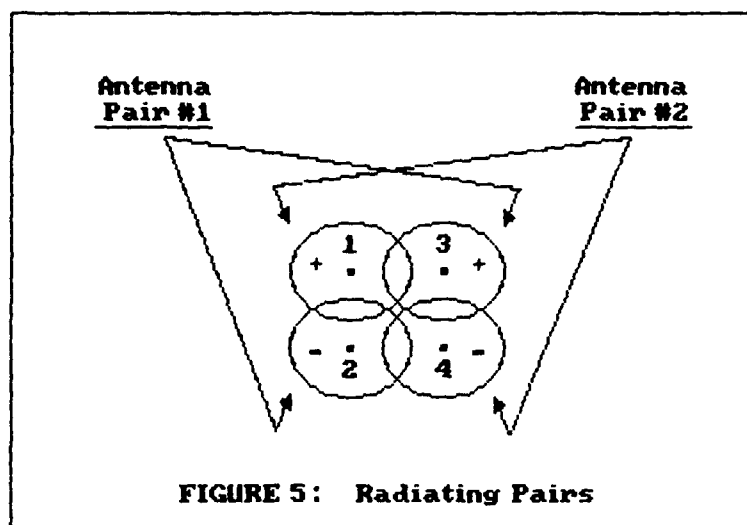
In KCVOR certain data are defined by the model. These are: time, position of the observation point, audio and carrier phase of the VOR reference signal as described above, the carrier frequency, the frequency of the VOR audio signals (30 Hz.), the speed at which the VOR signals propagate through space (the speed of light), and the locations of the VOR transmitting antennas. This information is defined in the program either explicitly in the form of declared constants, or implicitly in the form of logic flow.

The VOR variable signal is mathematically constructed from the transmissions of four isotropic point sources, where these point sources are models for the four Alford Loop antennas that compose the physical VOR transmitter array. Although this type of source is ideal and physically unrealizable, it provides an antenna pattern that results in minimal bearing error [14]. These transmitting elements are located symmetrically as shown in Figure 4, which is a typical configuration for a VOR array [15]. A Fortran Data statement is used to establish the locations of the point sources to the program.



With the antenna locations established, the constants initialized, and the aircraft in position, KCVOR proceeds as follows: First, the X-Y coordinates of the aircraft's position are determined. Then, the aircraft's distance from the origin is calculated, and, using this information, the distance from each antenna to the aircraft (observation point) is obtained.

Equations defining the formation of two "radiating pairs" out of the four point source antennas are calculated next. In an actual VOR system, there are two output lines from the goniometer which provide the audio modulation. The output on these two lines are identical except for a 90 degree phase shift at the audio frequency. One of the output lines is connected to antenna pair #1 and the other is connected to antenna pair #2. Equal amplitudes of the modulated signals are fed by the goniometer to each antenna pair. Further, each goniometer output is split equally and then passed through a half wavelength cable before being sent to one of the antennas in a pair, so that the relative phases



within a pair, at the carrier frequency, differ by 180 degrees, as indicated by the + and - signs in Figure 5 [16]. Calling  $CE_n$  the complex electric field transmitted by antenna "n", where CP1 represents radiating pair #1 and CP2 represents radiating pair #2, the program forms the two radiating pairs in the following manner:

$$CP1 = CE_1 - CE_3$$

$$CP2 = CE_2 - CE_4$$

where the minus signs account for the 180° phase shifts introduced by the half-wavelength cables.

## 2) Signal construction and sampling

KCVOR's main function is to calculate the phase of the VOR variable signal at a specified sampling location, because, as mentioned earlier, the phase (in degrees) of the variable signal is numerically equal to the VOR-estimated azimuth angle. The procedure to mathematically construct the variable signal is addressed here.

The composite received signal at the observation point is calculated by summing the complex-valued contribution from each of the four Alford Loop antennas. The phase relationship between the signals received from each of the antennas is proportional to the distance between an antenna and the observation point; the proportionality constant is the wave number. Because a far-field approximation is assumed, the  $1/R$  field strength dependence is omitted in calculations by KCVOR. Specific equations used by the model to determine the received VOR variable signal are given in Appendix A, along with a description of a method that normalizes distance values so as to minimize round-off errors by reducing the size of the complex-valued argument in the exponential function.

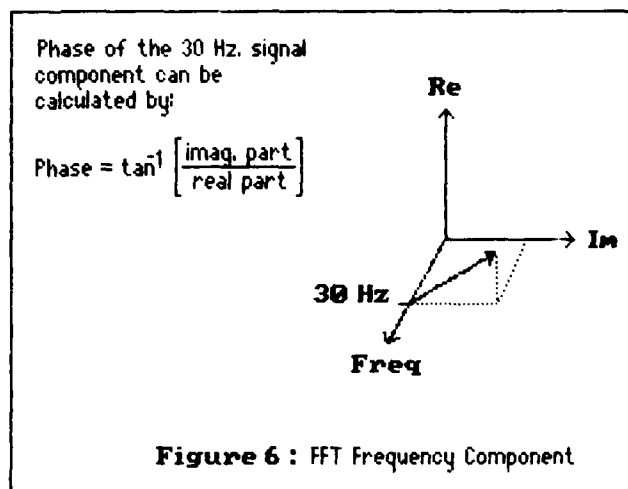
For each of the 5 degree azimuth positions sampled during a modeled orbit, a time-domain sequence of received variable signal values are generated for a period representing  $1/30$ th second, or one period of the VOR audio signal. The phase information used to determine VOR bearing is contained in this time-domain waveform. As is described in the following section, phase information is extracted from this computed waveform using a double precision, decimation-in-time, fast Fourier Transform (FFT) routine, which is resident in the model. In order for the sampled waveform to be compatible with the FFT input requirements,  $2^N$  equi-spaced samples are needed [17]. To provide the necessary resolution for this application, an  $N$  of 8 was selected, which corresponds to 256 time samples within the  $1/30$ th second interval. The

phase value returned by the FFT routine is then compared with the known azimuth angle to generate an error value for that observer position.

### 3) Signal processing

As mentioned above, a double precision, decimation-in-time, fast Fourier Transform provides the signal processing function for the model. A signal  $x(t)$ , where  $t$  stands for time, can be represented as a linear combination of a set of elementary time functions such as  $\sin(\omega t)$  and  $\cos(\omega t)$  [18]. When an FFT transforms a discrete time signal, such as the sampled VOR variable signal, into the frequency spectrum, it determines the complex-valued frequency components that were linearly combined to form that signal. All of the derived components are based on sine and cosine functions, with each part having an unique frequency, and an associated phase and magnitude [19]. It is the phase of the 30 Hz component of the variable signal that this model obtains from the FFT.

When the frequency spectrum of the sampled signal is output by the FFT, KCVOR only looks at the second component. The reason for this is that the first one is the D.C. component ( $\omega=0$ ), leaving the frequency of interest, 30 Hz., as the



next component. No frequency lower than 30 Hz. (trivial case of  $w=0$  neglected) was included in the mathematical signal construction. The real and imaginary parts of this 30 Hz. component can be used to determine the phase and magnitude of the VOR variable signal as it was sampled at the aircraft. But only the phase information is of interest, so only it is calculated. Figure 6 gives a graphical presentation of the information stored in a typical frequency component output by the FFT.

As is shown in Appendix A, where the mathematical construction of the variable signal is described, the variable signal is composed of a sine term and a cosine term. If such a function is input to the FFT with both phase terms set to zero [e.g.  $x(t) = \cos(\omega t + 0) + \sin(\omega t + 0)$ ], the phase of the frequency component depicted by " $\omega$ " is found to be -45 degrees, not 0 degrees as might be expected. In a VOR system, it is necessary that the variable signal and the reference signal be in phase on the zero-degree radial. Since the phase of the reference signal in KCVR is always zero degrees, the phase of the variable signal must be compensated so that it too is zero degrees on the zero-degree radial. This is done by adding 45 degrees to the value of phase obtained from the FFT ( $-45+45=0$ ).

In a physical VOR system, the tone wheel generates the reference signal, and the goniometer generates the variable signal. Although the two generated signals are isolated, both of the signal generators are mechanically coupled to the same synchronous motor (1800 rpm). Because the two devices are driven by the same motor, the initial phase

relationship between the two signals is determined by their relative positions on the motor shaft. So, to compensate for the 45 degree phasing problem mentioned above, the real world solution is to place the goniometer on the motor shaft so that it lags the tone wheel by 45 degrees [20].

#### 4) Error determination and output

In this final step, KCVOR has calculated the phase of the variable signal as determined by the FFT. The bearing angle is then calculated by:

$$\text{COURSE} = \text{VARIABLE SIGNAL PHASE} - \text{REFERENCE SIGNAL PHASE} + 45 \text{ DEGREES}$$

Since it is assumed that the phase of the reference signal is always  $0^\circ$ , the course is simply the phase of the variable signal plus  $45^\circ$ .

KCVOR next determines the error between the computed azimuthal position of the observation point and the point's actual position. The calculated bearing angle is subtracted from the "true" bearing angle to get the error incurred in the VOR signal transmission process. The true bearing angle is determined from the origin of the coordinate system, which represents the center of the VOR site, and the location of the observation point, which represents the position of the aircraft. Since the program specifies the location of all observation points, it knows their true location as accurately as the computer's double precision arithmetic. The error, the true bearing angle, and the calculated bearing angle are then output to the user. After this loop

is executed 73 times, a plot of bearing error versus true radial position is generated. The program then terminates.



### C. Theory of Operation for the "General VOR Model" (program GVOR)

The VOR model described here is designed to predict the bearing errors in a VOR navigation system due to parasitic scatterers in the vicinity of that system. The model has two distinct parts:

- (1) An unmodified version of the Numerical Electromagnetics Code (NEC-2) is used to model a VOR antenna element and to calculate its far field radiation pattern. Small parasitic scatterers, such as antennas, antenna masts, guy wires, or other conductors of arbitrary shape, are simulated near the antenna element, whereupon NEC-2 calculates the modified radiation pattern due to the interactive effects of the VOR antenna and the parasitic scatterers. This code uses the method of moments to obtain the desired solutions [21]. To model the effects of a scatterer on VOR system accuracy, each loop antenna is sequentially modeled in the presence of the scatterer, and field data are recorded for a far-field orbit around the source-scatterer configuration; this process is repeated for each of the four loop antennas thus providing complete information about complex path loss between each loop antenna and the observation point in the presence of the scatterer.
- (2) A FORTRAN program, called GVOR, reads the output generated by NEC-2 to obtain the pertinent scattered-field data. Then, for each observation point along the orbit, GVOR combines these data into the signal of a VOR antenna array, and then determines the navigation information present in the signal. This is done by

applying the appropriate time varying phasing between the output of the four Alford Loop Antennas (as provided by NEC-2), and then using an FFT to determine the phase and distortion of the received signal. If scatterers are present in the NEC-2 part of the model, then their effects on an ideal VOR signal are evident in GVOR's output. This output consists of the "true" azimuth angle as defined by the model, the calculated azimuth angle (which is based on the FFT's output), and the error between the two. A code listing of GVOR is given in Appendix B.

These two parts of the VOR model are discussed in the following sections, along with the assumptions made in the modeling process. The key points addressed include: some features and limitations of NEC-2, the modeling of conducting structures, approximations for modeling the Alford Loop antenna (which involves attempts at surface patch excitation), representation of the ground plane, and the VOR modulation scheme.

## 1. NEC-2 -- Part One of the "General VOR Model"

### a. The Numerical Electromagnetics Code (NEC-2)

The Numerical Electromagnetics Code (NEC-2) is an interactive FORTRAN program designed to model the response of antennas and other conducting structures due to electromagnetic field excitation. Wires and smooth surface geometries are used to model arbitrary structures in free space or over a ground plane [22]. NEC-2 uses the method of moments to numerically solve integral equations that determine the currents induced

on conducting structures by both direct waves and scattered waves. After calculating the currents on a structure, NEC-2 can determine, at an arbitrary observation point, the electromagnetic fields radiated by that structure, regardless of whether the current was induced by a direct wave or by a scattered wave (see Figure 7) [23]. These structures, which may be excited or parasitic, are specified by the user to the program by means of "data cards". A data card may include such information as the XYZ space coordinates of a structure component, or may specify a method of excitation, such as an incident plane wave or voltage source on a wire. A data card may also specify the type of output to be generated; this may include current and charge density on a conductor, electric or magnetic fields near a conducting structure, or radiated fields at observation points in space [24].

NEC-2 uses an integral equation approach to solve for unknowns and is generally not suitable for simulating a scattering structure that has dimensions larger than several wavelengths. This limitation exists because, in the numerical solution of the integral equation, as the size of a structure increases linearly, the number of unknowns generated by that structure increases exponentially (by about a factor of  $N^2$ ). Hence, while modeling a very large structure is theoretically possible, solution of the generated matrix equation may require more computer resource than is practical. Consequently, NEC-2 is not an efficient code for simulating a conducting structure that has dimensions larger than several wavelengths [25].

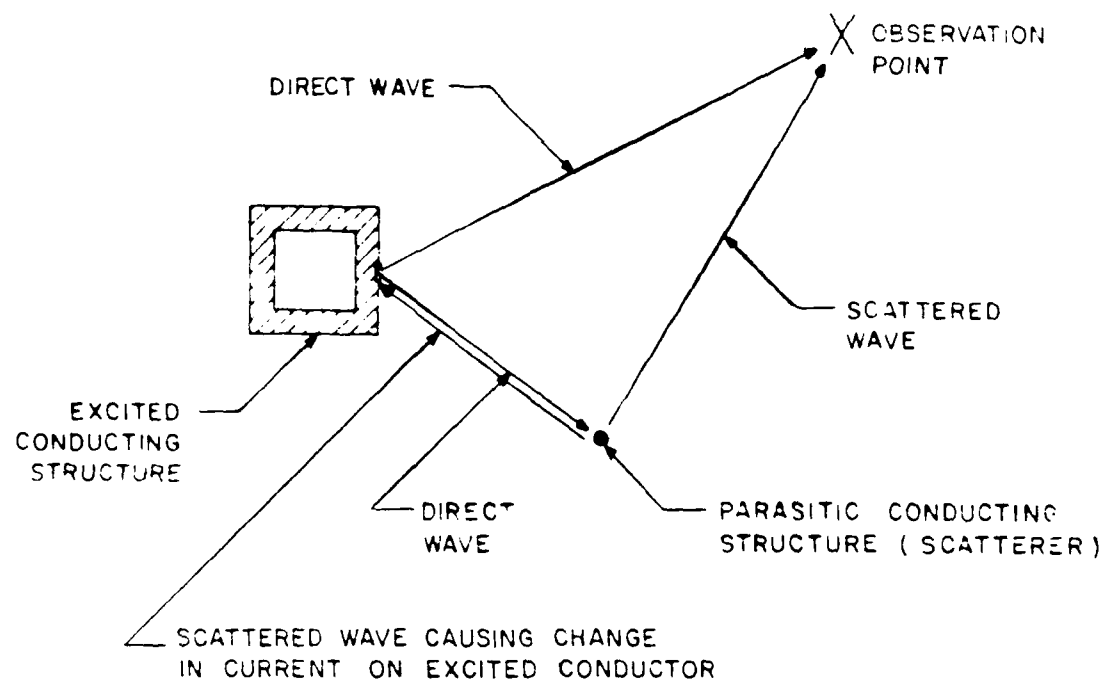


Figure 7: Observed field consisting of direct and scattered waves.

### b. An Overview on Modeling Conducting Structures

NEC-2 offers two options for modeling structures: (1) surface patches, and (2) wires. The user may model any structure that can be represented by surface patches and/or wires since the program combines an integral equation for smooth surfaces with an integral equation specialized for wires [26].

Small flat surface patches may be used to model conducting surfaces. Patches should be specified so that they completely cover the surface to be modeled, and, if chosen small enough, may be used to approximate curved surfaces. The program identifies a patch by the XYZ coordinates of its center, by the components of the outward-directed, unit normal vector, and by the patch area. Surface patches are generally restricted to the modeling of voluminous objects (closed surfaces), since patches only model the side of the surface from which their vector normals are directed outward [27].

In wire modeling, a wire may be composed of one or more segments, and is defined by the XYZ coordinates of its two end points and by its radius. To model a structure using wires, wire segments should geometrically follow the contours of the structure being modeled as closely as possible, using a piece-wise linear approximation for curved sections; a wire grid may also be used, in place of patches, to model flat surfaces [28].

A grid of wires appears electrically equivalent to a thin surface conductor if the grid spacing is small compared to the incident field

wavelength. For example, most microwave ovens have a glass door on the front through which the cooking food may be viewed. This glass door is embedded with a wire grid, or screen, while the other five walls of the cooking compartment are made of metal. If the size of the screen mesh is small with respect to the wavelength of the microwaves, which they are, then the screen will reflect the microwaves just as effectively as the metal walls. That is, a grid of wires can have the same electrical characteristics as a thin sheet of metal, the determining factors being the grid spacing and the wavelength.

As an example, suppose the sheet of metal in Figure 8 is to be modeled using the NEC-2 wires option. The first step is to have wire segments follow the outer boundaries of the sheet in a piece-wise linear fashion. Then, construct the interior of the sheet as a grid of perpendicular wires (as shown in Step 2 of Figure 8), with the distance between the wires much less than the wavelength of the incident electromagnetic field.

### c. Modeling VOR Components Using NEC-2

#### (1) The Alford Loop Antenna

A VOR antenna array is composed of four Alford Loop antennas. These four antennas are positioned as shown in Figure 9, with the antennas represented as squares. One of the first assumptions the model makes is that an Alford Loop antenna can be approximated by an excited, square

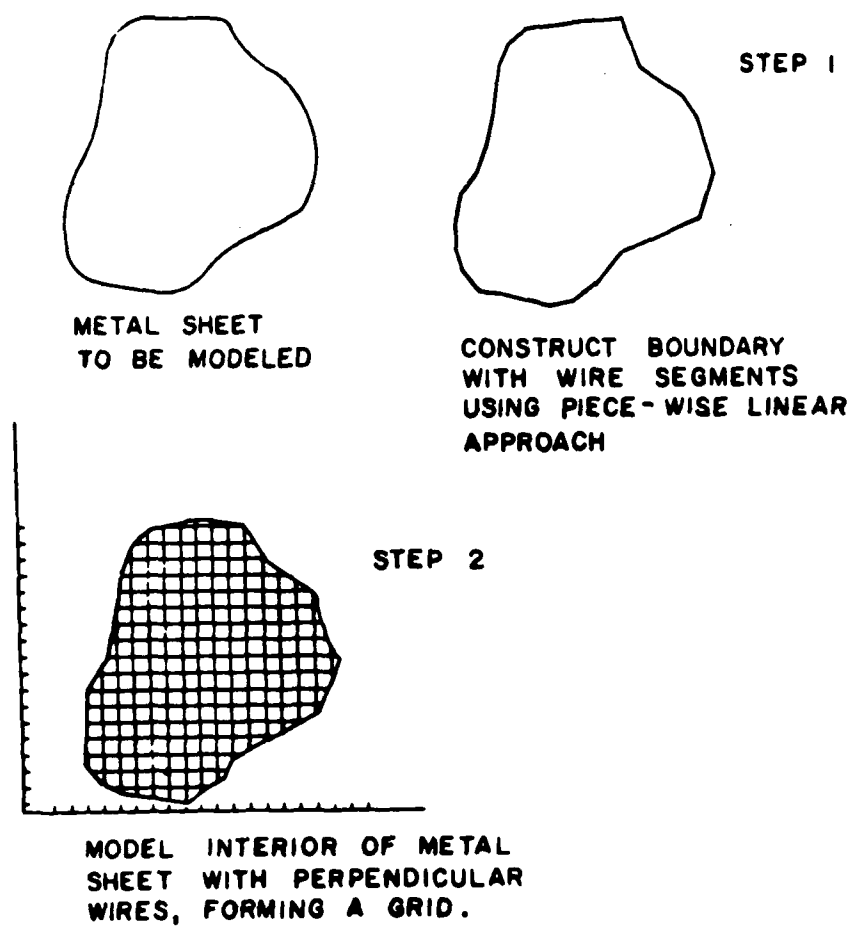


Figure 8: Modeling a sheet of metal with a wire grid.

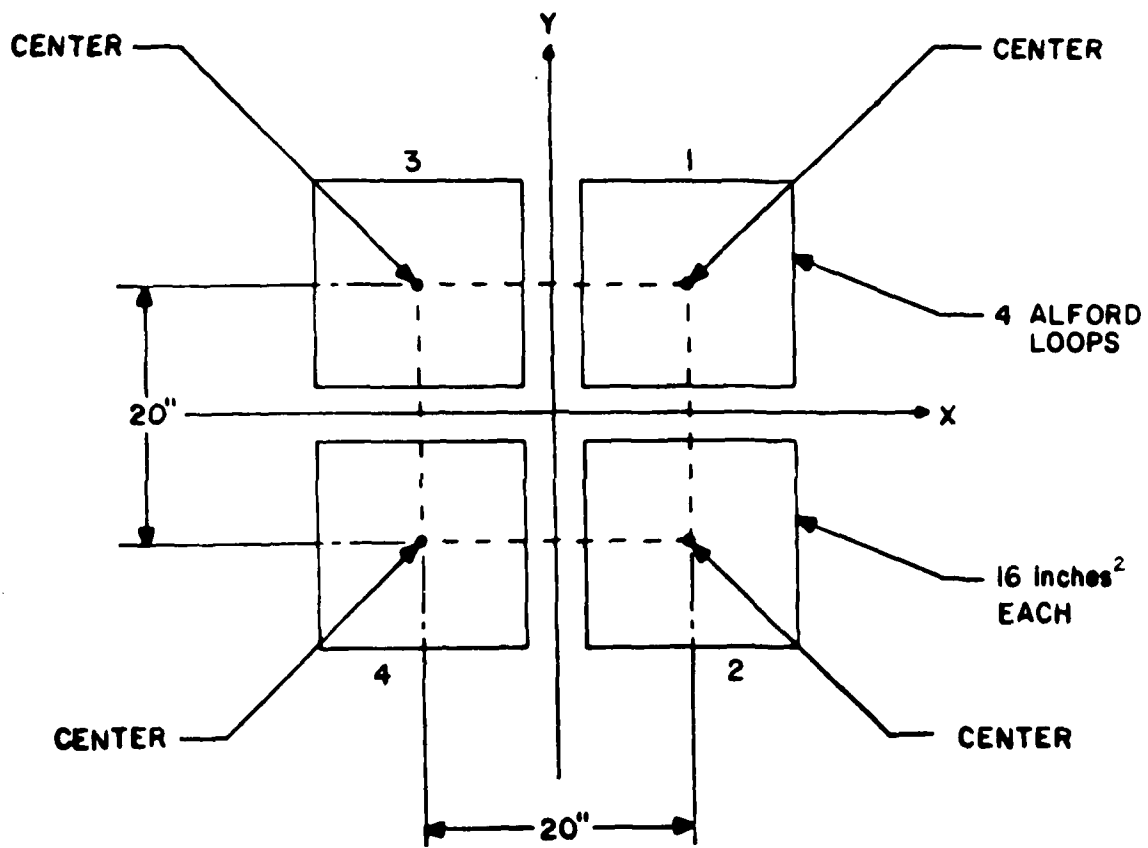


Figure 9. Relative antenna positions in physical VOR array.



loop of thin wire. This assumption is based on the fact that the Alford Loop is designed to approximate the circular radiation pattern of an ideal square loop antenna [29]. Although an ideal square loop is not physically realizable, NEC-2 can model it. And so, as a first attempt, a square loop of thin wire with the approximate the physical dimensions of the Alford Loop (about 20 inches per side) was input to NEC-2. However, the resulting output showed non-uniform current around the circumference of the loop.

In an actual Alford Loop antenna, the distribution of capacitance and inductance on the structure of the antenna enable the current distribution to be constant along the circumference, resulting in the desired circular radiation pattern. Clearly, a thin wire of the same dimensions as the Alford Loop antenna will not have the same current distribution, and hence will not have the same radiation pattern [30].

Previous efforts with NEC-2 aimed at modeling antennas indicate that realistic current distributions can be achieved using the actual dimensions of the antenna structure [32], [33]. However, the focus of this study is to investigate the performance of the VQR in the presence of parasitic scatterers, rather than the radiation pattern of the Alford Loop antenna, which is known to be circular. Thus, a study was undertaken using NEC-2 to determine a simpler, yet realistic, model approximation for the Alford Loop antenna. The most obvious simplification was to approximate the Alford Loop antenna by a smaller loop, constructed from thin wires. Such an antenna would produce the desired circular radiation pattern, although important questions about

the applicability of this approximation needed to be addressed, as is listed below:

- (1) Will a loop modeled smaller in radius than the physical radius of an Alford Loop interact with a scatterer in the same way as a loop modeled with the same dimensions of an Alford Loop? That is, even though the different size loops may give identical radiation patterns in the far field, will they continue to do so in the presence of scatterers?
- (2) How small should the modeled loop be? What loop size is needed to maintain a constant current around its circumference.
- (3) Will a loop modeled as a very thin wire (basically two dimensional) react to scatterers in the same manner as the four inch wide Alford Loop (three dimensional)?

To answer the first question, two loops differing appreciably in radius were used in the following experiment. First, one of the loops was excited and placed near a scatterer. The far field radiation pattern of that loop was then recorded. Next, the other loop antenna of different size was placed in the same position relative to the scatterer as was the first antenna and its far field radiation pattern recorded.

For this experiment, a horizontally polarized, parasitic scatterer was placed in the near field of (1.4 meters away from) an excited square loop of thin wire. The loop had a radius of 0.1 meters and was oriented in the horizontal plane. The resulting radiation pattern was observed

in the far field of the horizontal plane. Each modeled observation point was six nautical miles from the center of the square loop, and was rotated five degrees from the previous point, thereby forming a circle of observation points in the XY plane, six miles in radius. Keeping the scatterer in the same position, the square loop was replaced with one that had a radius of 0.007 meters. The same observations as for the larger loop were made and recorded. The two sets of data were then run through a cross-correlation program, with the resulting correlation coefficient being 1.0, indicating that the data were identical. Conclusion: according to NEC-2, the two above configurations yield identical far-field results; consequently, it would be appropriate to use the small loop approximation in this application of NEC-2.

In regard to the size of the modeled Alford Loop antenna, it is important that antennas used in a VOR navigation system have a circular radiation pattern because this relates to bearing error. A thin, square loop antenna gives a circular radiation pattern only if the radius of the loop is less than 0.05 times the exciting wavelength [33]. A circular radiation pattern from a thin-wire, square-loop antenna is a direct result of having constant current around the loop, which in turn is the result of the loop being small. As the size of one of these loops is increased, the current does not remain constant, but starts to vary sinusoidally around the loop, thus distorting the circular radiation pattern. The radius of a thin-wire, square loop that approaches the physical dimensions of an Alford Loop would be approximately 0.254 meters. The VOR frequency modeled has a wavelength

of 2.72 meters, giving a small loop condition of  $(0.05 * 2.72 =) \underline{0.136}$  meters. So, as mentioned previously, a square loop of wire with the same circumference as a physical Alford Loop does not give a circular radiation pattern since the actual dimensions are considerably greater.

NEC-2 was used to determine the radiation patterns and current distributions of several "small" square loops of thin wire. Modeled loop radii were varied from 1.0 meters to 0.007 meters. For loops 0.01 meters in radius and smaller, the modeled current was constant around the circumference. Figures 10-A, 10-B, and 10-C show the results for the largest of the six small-loops modeled. The data points denoted by x's correspond to a loop radius of 0.1 meters. (The x's on the Current Phase Distribution graph are partially hidden on the "Current Phase = 90 degrees" line). It should be noted that this is the first loop, from larger to smaller, to cross the 0.136 meter small-loop boundary, and that it is also the first loop to give approximate straight lines on both the Current Magnitude Distribution and the Current Phase Distribution, indicating an approximate constant current condition. Based upon these results, a square loop with a side of 0.2 meters (0.1 meters radius) was chosen as being appropriate for VOR modeling purposes.

The remaining question is whether a loop of thin wire will react to scatterers the same way as the approximately four inch wide Alford Loop antenna. To answer this question, an attempt was made to model an Alford loop antenna in three dimensions, resembling a square doughnut,

# Current Magnitude Distributions on Small Square Loop Antenna

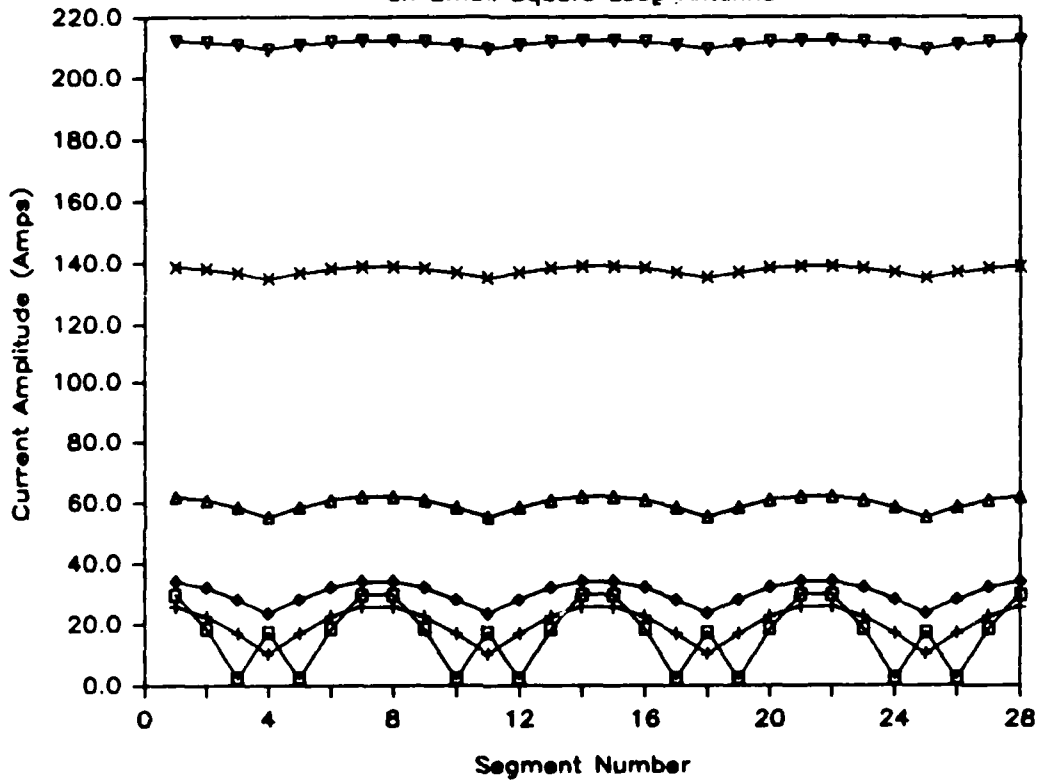


FIGURE 10-A

# Current Phase Distributions

on Small Square Loop Antenna

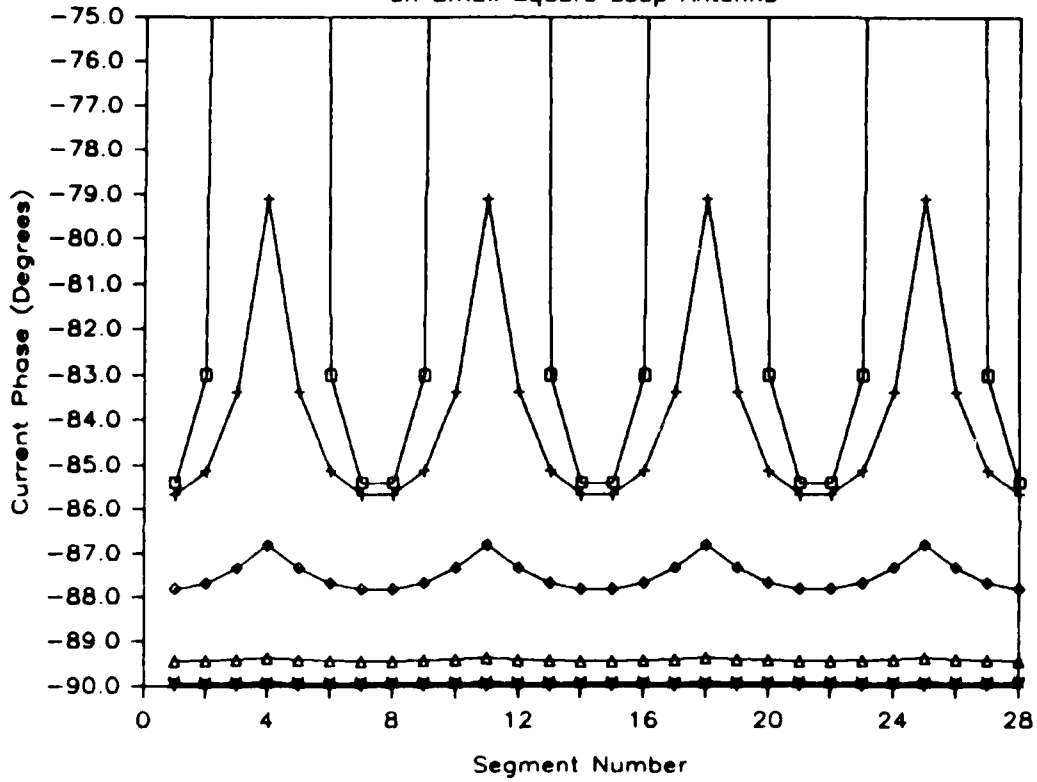


FIGURE 10-15

# LEGEND

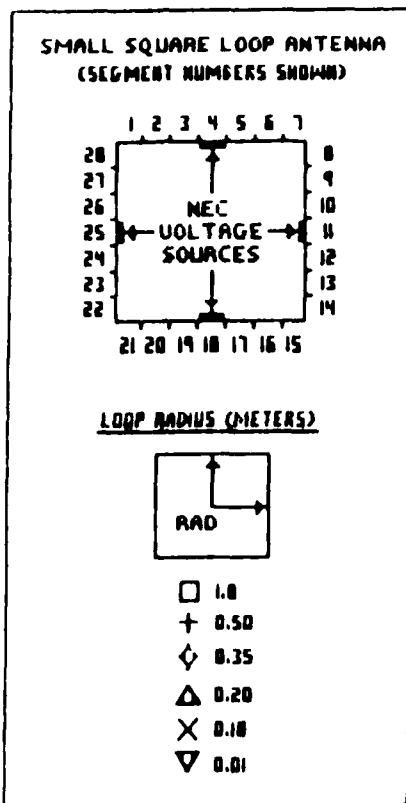


FIGURE 10-C

using the NEC-2 surface patch feature, with the added third dimension representing width. Voltage sources were provided by attaching excitation sources to selected patch centers as described in the NEC user's manual [34]. These patches were chosen so as to give the antenna a geometrically symmetrical excitation, and the excitation sources were placed in the interior of the doughnut. (NEC-2 requires voltage source excitation of patches by connecting source wires to patch centers.) Without modifying the NEC-2 program, only ten voltage sources are allowed in any given program execution. In order to get a circular radiation pattern from this square doughnut loop, the excitation current must be constant around the outer surface of the loop. However, ten voltage sources were not sufficient to provide this constant current condition, even on a very small doughnut. Further, one of the goals in using NEC-2 for VOR modeling was to not modify the NEC code in any way. It was desired to use this standard software package without modification so that the software would not have to be validated again. For these reasons, the three-dimensional, "wide", Alford Loop model was abandoned.

The primary difference between using a thin wire approximation for the Alford Loop and using a more realistic "wide" antenna model as described above, is that the wire model accounts for currents only in the axial direction of the wire, whereas a wide antenna model made of surface patches would account for axial currents and transverse currents [35], both of which are found on an actual antenna. If transverse currents are present, they generate electromagnetic fields that interact with



scatterers and may be significant at the observation points in the far field. However, these fields are vertically polarized and are typically small in magnitude compared to the horizontal components. In addition, in a VOR navigation system, the airborne VOR receiving antenna is horizontally polarized so that the vertical components of the received signal are approximately 30 dB down from the received horizontal components [36]. Hence, the receiving antenna effectively filters out vertically polarized waves. This suggests that ignoring transverse antenna currents in the model does not affect model accuracy, even if these currents are comparable in magnitude to the axial currents, which they are not. Consequently, the omission of transverse antenna currents in modeling VOR bearing error does not degrade model results.

The experiments using NEC-2 described above indicate that approximating the Alford Loop antenna by a thin-wire loop of smaller dimensions is reasonable for the application being addressed. Accordingly, a square loop antenna, 0.014 meters on a side, comprised of wire elements 0.0005 meters in radius, was used to generate the model results presented in subsequent sections of this report.

## (2) The Counterpoise

In a VOR system, a finite counterpoise is typically located ten feet above the earth, and is intended to act as a ground plane for the VOR transmitting antennas. The VOR antennas are usually positioned 4 feet above this counterpoise, and thus 14 feet above ground level [37]. One of the assumptions made in the model is that the counterpoise can be

represented as an infinite ground plane. That is, in the model, the counterpoise is approximated by an infinite, perfectly conducting ground plane located at ground level. In a physical VOR system, it is the counterpoise that is attempting to approximate an infinite ground plane. The antennas of the model are located 4 feet above this counterpoise, which in this case, is four feet above the ground. If it is desired to model a 46 foot tower in the vicinity of the VOR, the first 10 feet of the tower up from ground level are omitted since this is the amount of tower that would be below the counterpoise in a physical system.

### (3) The VOR Modulation Scheme

A VOR antenna system is composed of an array of four Alford Loops being fed in a time-varying amplitude and phase relationship. The General VOR model is designed to calculate the received fields from each of the four antennas individually, to include the effects of parasitic scatterers on each antenna's radiation pattern using NEC-2, and to subsequently combine those fields according to the VOR modulating scheme (GVOR), thus simulating the performance of a VOR in the presence of parasitic scatterers. The VOR modulation scheme is the method used to generate the rotating limaçon pattern that is indicative of the VOR variable signal.

The first facet of the modeling job is performed by NEC-2, and its goal is to assemble the data file that program GVOR processes in the second part of the job. This data file consists of the calculated fields for each of the four antennas, scattering effects included. The excited

antenna has a radiation pattern and so does the parasitic scatterer, and NEC-2 calculates these patterns. Actually, NEC-2 calculates the field at user-chosen observation points, not the radiation pattern, although the radiation pattern can be obtained from the calculated fields of many such points. Once the fields from the antenna and the scatterer are calculated for a chosen observation point, NEC-2 uses the superposition principle to determine the resultant fields at that point.

In order to simulate the VOR, the NEC-2 program is run four consecutive times, once for each antenna in the VOR array. All four executions of NEC-2 use the same input data (such as frequency, excitation voltage, data output formats, scatterer location, etc.) except for the position of the square loop antenna. The antenna position is changed each time so that each "program run" analyzes the output of only one antenna in the four antenna array. Figure 11 shows how the modeled Alford loop is positioned for each of the four executions of NEC-2. As in program KCVOR, GVOR analyzes the VOR system at 73 observation points, once every five degrees around the VOR, 0 through 360 degrees inclusive. Since GVOR uses NEC-2's output, these 73 observation points are chosen for NEC-2 field calculations each time NEC-2 is run. These points form a circle in the far field, with the center of the circle being the center of the antenna array.

#### d. Description of the NEC-2 Output File

The output for a single run of NEC-2 contains more information than is needed for modeling the VOR. At the conclusion of the execution of NEC-

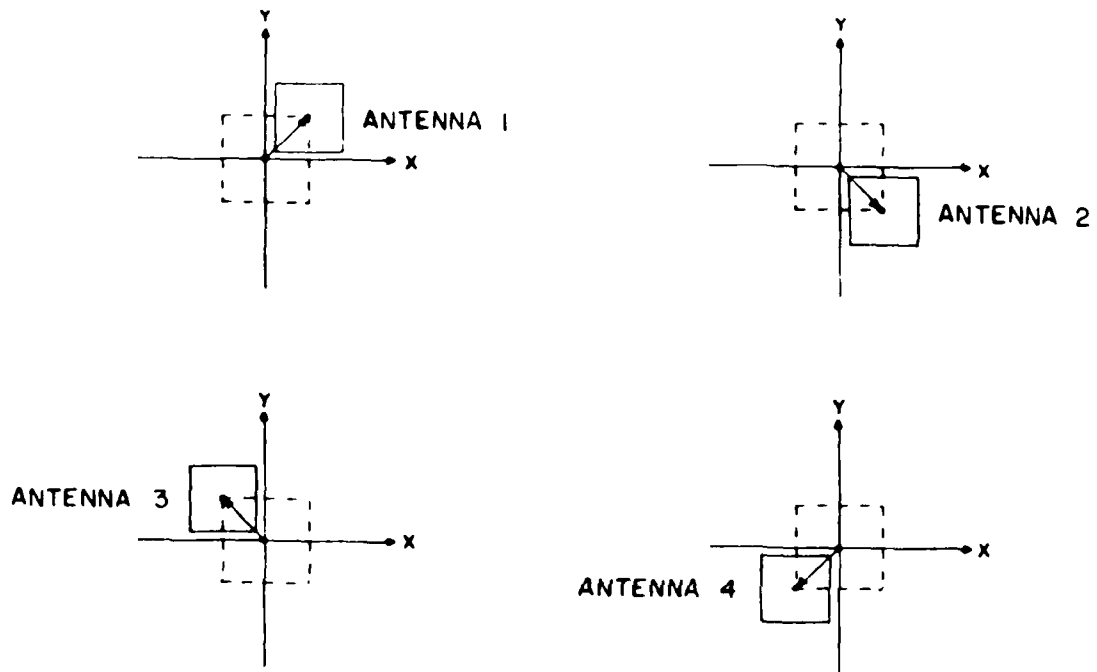


FIGURE 11: Modeling the VOR Antenna Array with NEC-2

2, the entire output file is written to a disk file called "NEC.DAT". Since NEC-2 is executed four times in the course of the VOR model, NEC.DAT eventually contains four similar blocks of data (4 NEC-2 output files), with the difference between files being that each data block is based on a different antenna location. The following is a sequential description of what one NEC-2 output file contains:

- (1) A user-entered comment section.
- (2) A structure specification section that echos the information given to the program as input. This includes the XYZ coordinates of the beginning and ending points of each wire specified. Accompanying each set of coordinates is the tag number (name) of the wire and the number of segments that the wire is divided into. If a structure has been moved, the coordinates that were listed on the Move Data Card are also given.
- (3) The final coordinates of all segment centers are given along with each segment's length and radius. A map is also given telling, by absolute segment number, which wires have common end points.
- (4) All other data input to the program are also listed in the output file. Examples are: which segments were excited by a voltage source and the magnitude of that excitation; the frequency of excitation; the format parameters for calculated values that are to be output; whether or not a ground plane was specified, and, if so, what type.

- (5) A section on antenna input parameters which gives the voltage, the current, and the impedance of each excited segment.
- (6) A section that tells the current on each segment, regardless of whether it was induced or excited.
- (7) A section that states the range to the observation point. If the observation point is incremented through a series of angles, the range is an indication of the absolute distance to each observation point.
- (8) A section that gives extensive information on the radiation patterns at the chosen observation points.

## 2. Program GVOR -- Part Two of the "General VOR Model"

The part of the NEC-2 output file on radiation patterns, which is described in section (8) under "Description of the NEC-2 Output File", is reproduced as Table 1. Each row of information in this table gives data for one of the 73 observation points, where the data describe the complex electric field at the observation point due to one of the four VOR antennas. For example, Table 1 might represent all of the observations made on antenna #1. The format of this output is dependent on the data input to NEC-2, with Table 1 being typical for a run of the General VOR model. Notice the first column labeled "ANGLES". The observation points have a constant angle of elevation, theta. However, the angle phi, which represents the azimuth angle, is stepped in five degree increments, full circle around the origin, for a total movement of 360 degrees and a total of 73 data points.

The NEC-2 contribution to the VOR model is the calculation of the horizontal components of the complex electric fields in regard to the far field radiation patterns of each of the four elements in the VOR antenna array. These calculations account for the interactive effects of a specified scatterer(s) on the radiation pattern of each antenna. This information, for one of the antennas, is listed in the last column of Table 1 and is labeled "E(PHI)". When GVOR reads NEC.DAT (the disk file containing the NEC-2 output) the vertical components of the radiated electric fields, E(THETA), are neglected. This is because, as mentioned earlier, airborne VOR antennas are horizontally polarized, which means that these "real world" antennas effectively ignore the

vertical components of VOR signals. The "POLARIZATION" and "POWER GAINS" columns are also extra information and are neglected by GVOR. Only the PHI Angles and the magnitudes and phases of E(PHI) are of interest to GVOR.

**a. The NTG (NEC To GVOR) Subroutine**

NTG is a subroutine of GVOR that provides the interface between NEC-2 and GVOR. NTG scans the NEC.DAT disk file for the keyword "POLARIZATION" (see Table 1), which appears in the range of certain columns only four times in the entire file -- once for each antenna. When NTG finds this keyword, it knows it has found the radiation pattern data for one of the 4 elements in the VOR antenna array. Of these data, only the azimuth angles of the observation points and the horizontal components of the electric fields at these observation points are of value in modeling the VOR. Therefore, NTG reads the PHI angles and the magnitudes and phases of E(PHI) from the disk file, and then stores this information in the host computer's memory (as variable arrays) for future access by GVOR. This process is repeated for each occurrence of "POLARIZATION", so that when GVOR regains control from NTG, it has access to the fields radiated by all four antennas, as calculated by NEC-2. It should be noted that the effects of parasitic scattering are inherent in the field information at this point. The remaining task for GVOR is to process this information in such a way that it looks like the output of a VOR antenna array, rather than the output of four individual antennas. This is done similar to the way that program KCVOR constructs the VOR variable signal, which is described in the section "Theory of



Operation for the Basic VOR Model". But GVOR does do some things differently, and those differences are discussed below.

#### b. Processing the NEC-2 Data

When NTG retrieves the data from NEC-2, it retrieves 4 sets of 73, 73 observation points for each of four antennas. As the VOR signals are constructed, GVOR accesses these data as 73 sets of 4. It takes the output of all four antennas for a particular observation point, and provides the time-varying amplitude and phase relationship necessary for a VOR signal.

The horizontal components of the radiated, complex, electric fields are output by NEC-2 in polar form. Fortran-77 handles complex numbers in Cartesian form, so GVOR's first processing task is performing a polar to rectangular conversion on all the retrieved fields data. After this is done, the main program loop is entered for one of 73 executions. Here, the VOR signals are constructed for one of the observation points by using the output of the four individual antennas simultaneously.

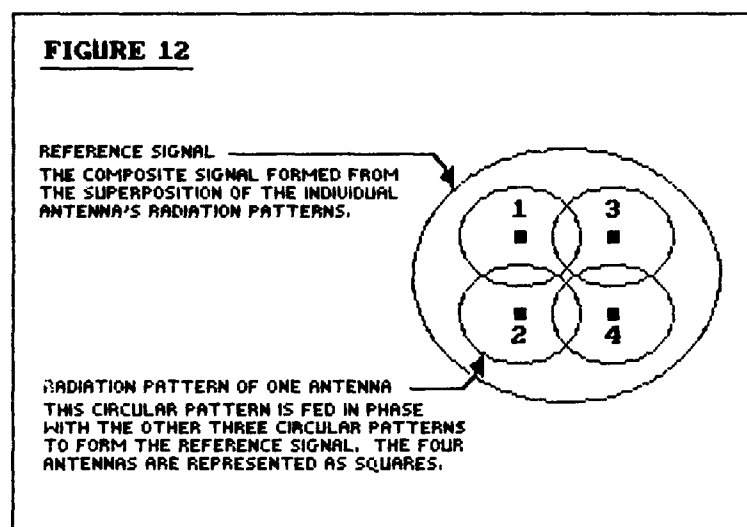
GVOR calculates the observation points that were input to NEC-2. Hence, before it begins signal construction for a particular observation point, it compares the expected azimuth angle with the value that is read in by NTG, to ensure that the data retrieved are the data expected. If the angles do not match, an error message is sent to the user and program execution is terminated; otherwise, processing continues. It should be noted that up to this point the main difference between programs GVOR

and KCVOR is that GVOR obtains its information on the VOR antenna fields from NEC-2 (scattering included), whereas KCVOR calculates this information itself (scattering not included).

As the processing continues, signal construction and analysis of the VOR variable signal is conducted in the exact same way as it is in program KCVOR. Although the antenna fields are supplied to GVOR by NEC-2, these antenna outputs are phased together and analyzed with the same routines that are used in KCVOR; even the same FFT routine is used. The two programs differ, however, when it comes to the VOR reference signal.

In KCVOR, the radial distance  $R$  is subtracted out in the "normalization" of the signal path lengths for each antenna, and thus  $R$  has no effect on the phase of the VOR variable signal. So, all that KCVOR has to do in terms of the reference signal is to choose a phase for this signal so that the variable signal and the reference signal are in phase at 0 degrees azimuth (with respect to time =  $t_0$ ); there is never any need to construct the reference signal. In GVOR, however, the propagation paths are not normalized because NEC-2 handles all of the calculations for the radiated fields, thereby necessitating the construction of the VOR reference signal.

A VOR reference signal has a circular radiation pattern which is centered on the VOR, and although its phase varies with  $R$ , it is independent of the azimuth angle. Each antenna in the modeled VOR array possesses the characteristics of a VOR reference, except that its radiation pattern is not centered on the VOR. But if the outputs of the



four antennas are added together in phase, in the far field it appears as if the composite pattern is a reference signal centered on the VOR. And so this is how GVOR models the reference signal. When the four antennas are observed in the far field, they appear as one point source radiating from the origin. Figure 12 gives an idea of how symmetry helps in the construction of the reference signal.

GVOR calculates the reference signal's phase, and then proceeds to find the omnibourse of the observation point using the equation:

$$\text{COURSE [deg]} = \text{PHASE OF VARIABLE SIGNAL} - \text{PHASE OF REFERENCE SIGNAL} + 45$$

The addition of the 45 degrees accounts for the initial phasing of the tone wheel and the goniometer on the 30 [rev/sec] motor shaft. In a real VOR system, the tone wheel generates the reference signal and the goniometer generates the variable signal, and both of these devices are driven by the same motor as described previously. The initial phasing

between these signal generators is needed so that the reference signal and the variable signal are in phase at 0 degrees azimuth [38].

GVOR then proceeds to determine the error between the computed bearing angle of the observation point (the omnicoarse) and the point's actual position. The calculated bearing angle is subtracted from the "true" bearing angle to get the error incurred in VOR signal transmission modeling. The true bearing angle is known from the overall design of the program -- one observation point for every five degrees around the VOR. The azimuth angle of all observation points are exact multiples of 5 degrees, and the multiple that is of present interest to GVOR is already kept track of in the program because the antenna information retrieved from NEC-2 is indexed by "true" azimuth angle.

GVOR concludes one iteration of the main program loop by outputting the true azimuth angle, the derived azimuth angle (the omnicoarse), and the error between the two. This output is sent to the user in just the same way as it is sent from KCVOR.

### III. RESULTS

The results of the modeling effort are presented in the same sequence that the VOR model is presented. That is, first, the results obtained from model KCVOR are presented, along with explanation of how it was determined that this model operates properly. An understanding of KCVOR's results gives the reader the necessary background for interpreting the results of model GVOR. Next, the baseline output from GVOR (no scatterers) is presented and compared to KCVOR's output. Following is an evaluation of GVOR's performance with respect to measured data.

#### A. Model KCVOR

Model KCVOR shows itself to be operating properly by its correct estimation of octantal error and system response to variations in the VOR antenna patterns. Octantal error is an inherent and periodic bearing error that makes four cycles within the  $360^\circ$  of azimuth about the VOR array, with its name being derived from the presence of eight error peaks. Generally, octantal error is present to some degree in all VOR's, with  $\pm 0.6^\circ$  peak error not unusual. However, as is discussed later, octantal error is a controllable quantity, and KCVOR has verified that this error can be reduced to  $\pm 0.0004^\circ$  peak by using textbook antenna pattern values.

In the original KCVOR model, the horizontal radiation pattern of the Alford Loop antenna was assumed to be isotropic. However, due to a proximity effect in the actual VOR array, there are induced currents

caused by mutual coupling between antennas, which tends to alter the shape of the composite radiation pattern. In particular, the figure-eight pattern of a radiating pair (which is the composite pattern of two phased, individual antennas) becomes elliptical in shape, rather than circular. Octantal error results because the four lobes radiated from the two radiating pairs of a VOR array are non-circular. It is possible to cause the four lobes of the two figure-eight patterns to be more circular by making the individual VOR antennas radiate elliptical patterns, rather than their assumed circular patterns. The result is the minimization of octantal error. If the lobes can be adjusted so that they are perfectly circular, then octantal error will no longer exist [39].

When the original KCVOR output its first error curve, it was sinusoidal in nature, with eight peaks through the 360° of azimuth, with each peak  $\pm 0.55^\circ$ . This was recognized to be octantal error particularly since the peak modeled error values were typical for VOR facilities.

Reducing octantal error in an actual VOR usually involves a tradeoff, because other errors are often created in the process. However, created errors such as these are not a problem in a computer model since antenna patterns can be defined explicitly. Hence, a test for validation of the modeling concept was to reduce octantal error by specifying antenna patterns known to reduce this error.

In Appendix B there is a program listing called KCVOR-M, where the M stands for modified. The modifications that were made to KCVOR

introduced two "ellipse" factors, which, when multiplied by the individual antenna patterns, cause composite radiation patterns that are elliptical in shape. The purpose in doing this was to emulate the effects on Alford Loop radiation patterns that are achieved by adjustments to its endplates. These adjustments are known to affect the circularity of the radiation pattern, and are used by VOR technicians to reduce octantal error. In the model, one of the ellipse factors is applied to the antennas in radiating pair #1, and the other is applied to radiating pair #2. The program modifications were made so that the optimum ellipse factors could be determined. Since a circle is a special case of an ellipse, it also possesses an ellipse factor, as defined by model KCVOR-M, a factor of 1.0. It was found that lowering the ellipse factor for one antenna pair, and then increasing the factor for the other pair by the same amount, produced the desired effect. The two optimum ellipse factors that were found were in the neighborhood of AEF=0.9608 and BEF=1.0392. The modeled VOR system response to the variations in the antenna patterns by ellipse factors AEF and BEF was a reduction in octantal error from +/- 0.55° to +/- 0.0004°. The correct response of the model to variations in the Alford Loop antenna patterns, indicates that the modeling approach is valid.

## B. Model GVOR

### 1. Baseline model output (no scatterer) -- a comparison with KCVOR

Before introducing parasitic scatterers as another variable into the modeling process and attempting to accomplish all VOR model objectives

at once, attention was focused on mating KCVOR with NEC-2 to produce a general VOR model named GVOR. The initial goal was to generate results using GVOR, in the absence of parasitic scatterers, that would be comparable to the results obtained from KCVOR; namely, the output should show the presence of an octantal error curve approximately  $\pm 0.6^\circ$  peak. This section describes the results obtained from GVOR with no scatterers present.

Figure 13 shows the output obtained from GVOR when parasitic scatterers were not included in the modeled scenario. As seen in the figure, this is a typical octantal error curve, in shape and in magnitude with the peak error being  $\pm 0.51^\circ$ . This encouraging result compares well with KCVOR's result of  $\pm 0.55^\circ$  peak error, and indicates that the model is functioning properly in the absence of scatterers.

## **2. Modeled results of horizontally polarized parasitic scatterers and a comparison with measured data**

Figure 14 shows two parasitic scatterers that were modeled by GVOR. These structures, which are made of 3/4 inch diameter copper tubing, were chosen to be modeled because they were used in an earlier study to collect measured data from a VOR facility that had these scatterers on the radome of the VOR. This earlier study, entitled *Assessment of Correlation Between Second Generation VOR Monitoring and the VOR Signal in Space*, was performed by Ohio University's Avionics Engineering Center [40]. Data for this study were obtained for the purpose of determining the correlation between the near-field signals at the Remote Maintenance



# BEARING ERROR FOR MODELKCVOR

Baseline Output --- Dotantal Error Curve

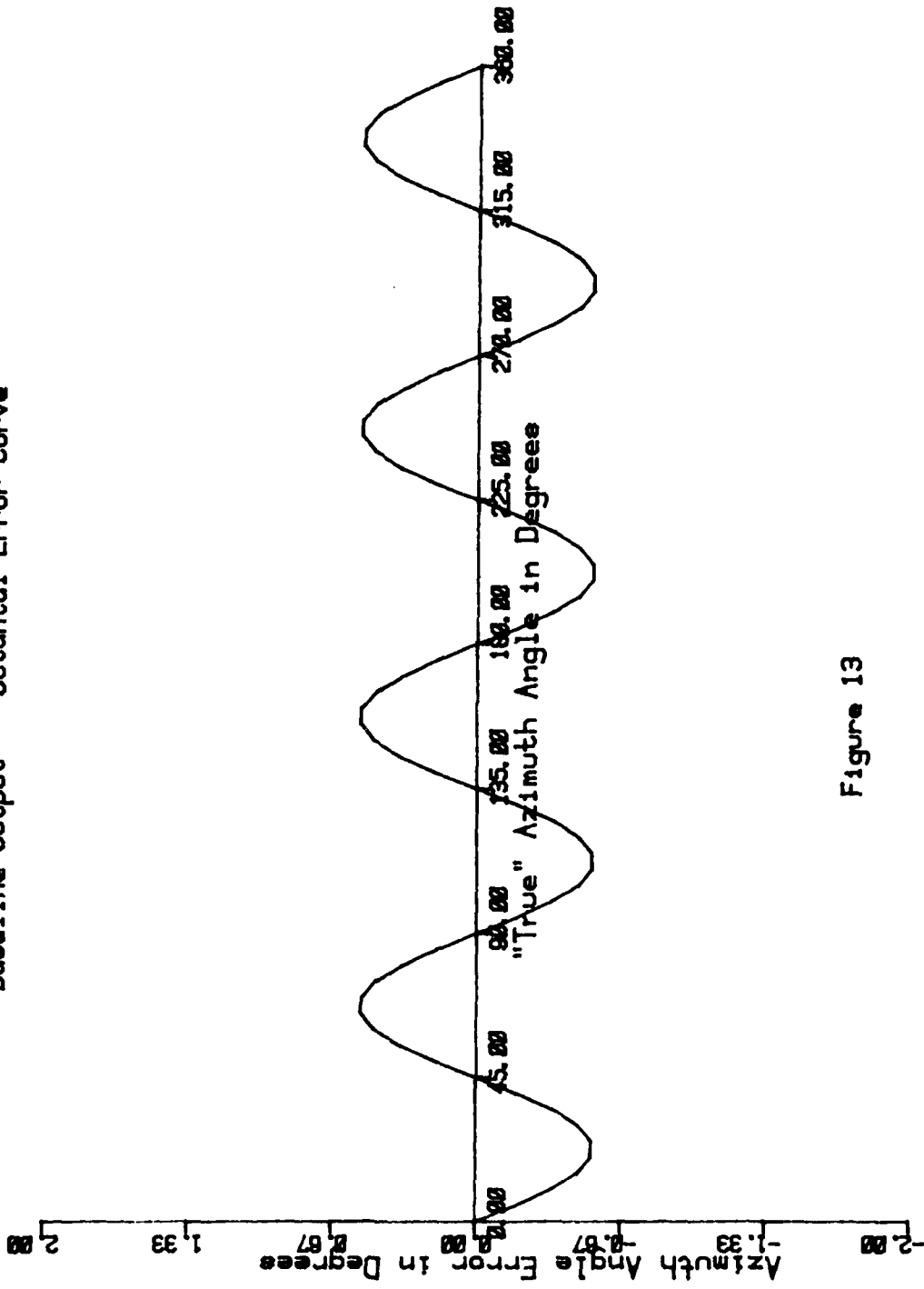
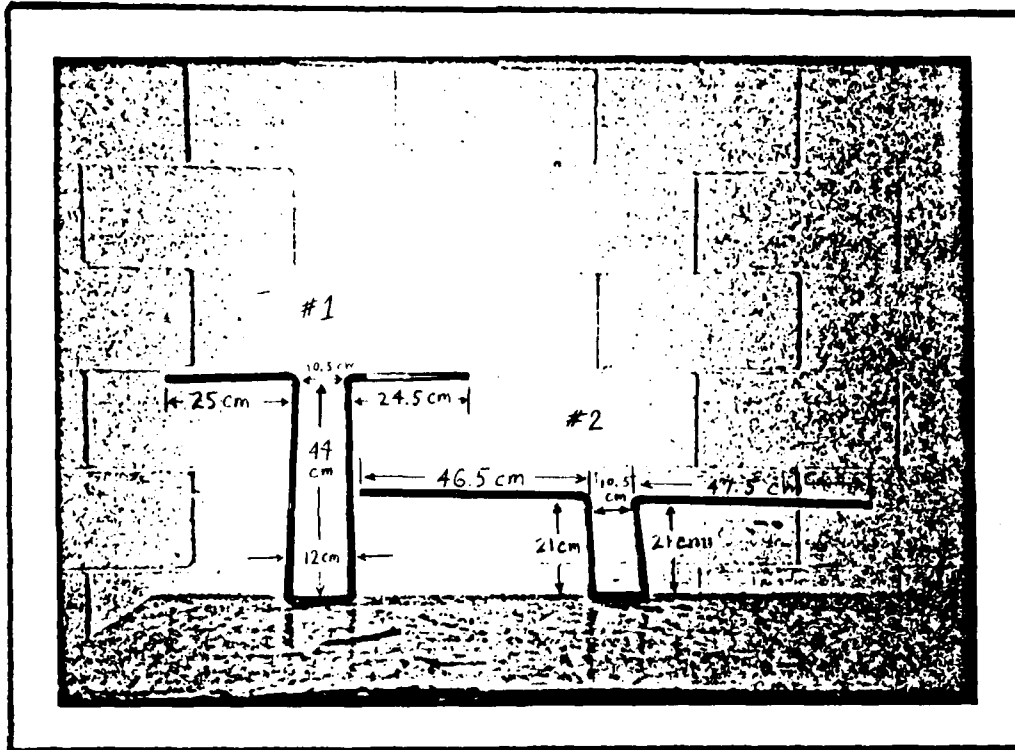


Figure 13



Two Parasitic Scatterers Modeled by GVOR

Figure 14

Monitor (RMM) system and the far field signals at an observation tower and at airborne locations.

The dimensions of the scatterers in Figure 14 were input to NEC-2 according to the conventions specified in the NEC-2 User's Guide for modeling wire structures. Only one scatterer was modeled at a time, and that scatterer was positioned relative to the VOR antennas as documented in the forementioned study. Measured airborne VOR data were collected with the scatterer placed on the VOR radome so that it was oriented horizontally. VOR error data were collected for the scatterer at various heights on the radome, and at different azimuth angles.

Figures 15 through 20 show modeled versus measured data. Each figure indicates which scatterer was used, where it was located, and the range of the observation points. Table 2 gives the peak to peak VOR error for each of the six figures and for each set of data in those figures. In Figure 15 the general trends and peak to peak values of the two measured data sets (RMM and tower) are about the same, and the modeled data shows just as much agreement. In Figure 16 the peak to peak values for the airborne and modeled data agree very well, while the RMM peak to peak value is substantially less; in regards to the trends (oscillations), the RMM data match up consistently with the airborne data, while the modeled data shows a little lesser agreement.

At this point, a few words are needed about the measured data. For Figures 15 through 19, the two sets of measured data in each figure theoretically should correlate highly; but, as can be seen, sometimes

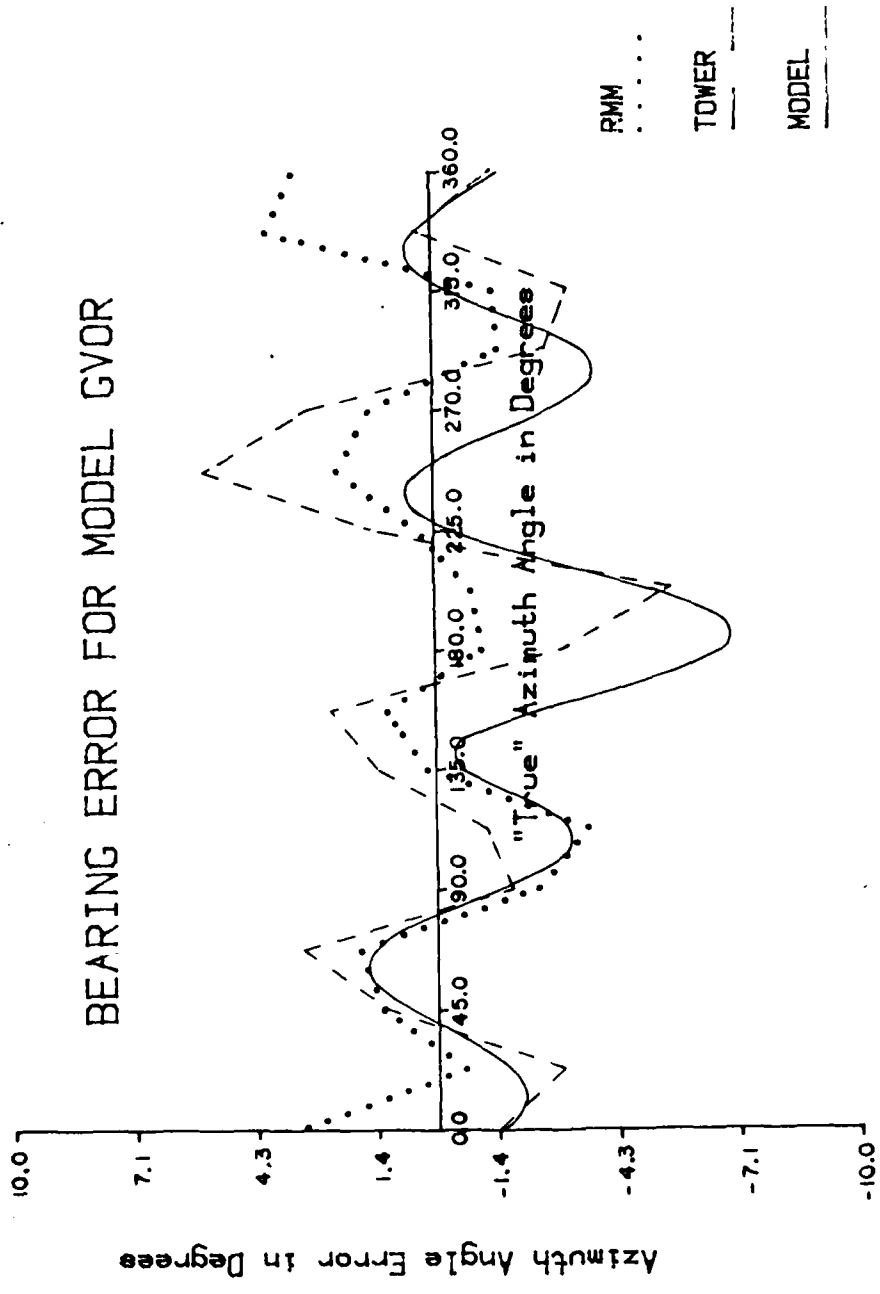


Figure 5 VOR errors due to parasitic scatterer No.(1): the scatterer was located on the 45 degree radial, mounted on the Radome, 72 inches above the counterpoise. The solid curve is model generated data. The dotted curve is data measured using the RMM system. The dashed curve represents data collected from a mobile tower, located 800 feet in radius from the VOR system. Theta = 89.00 degrees.

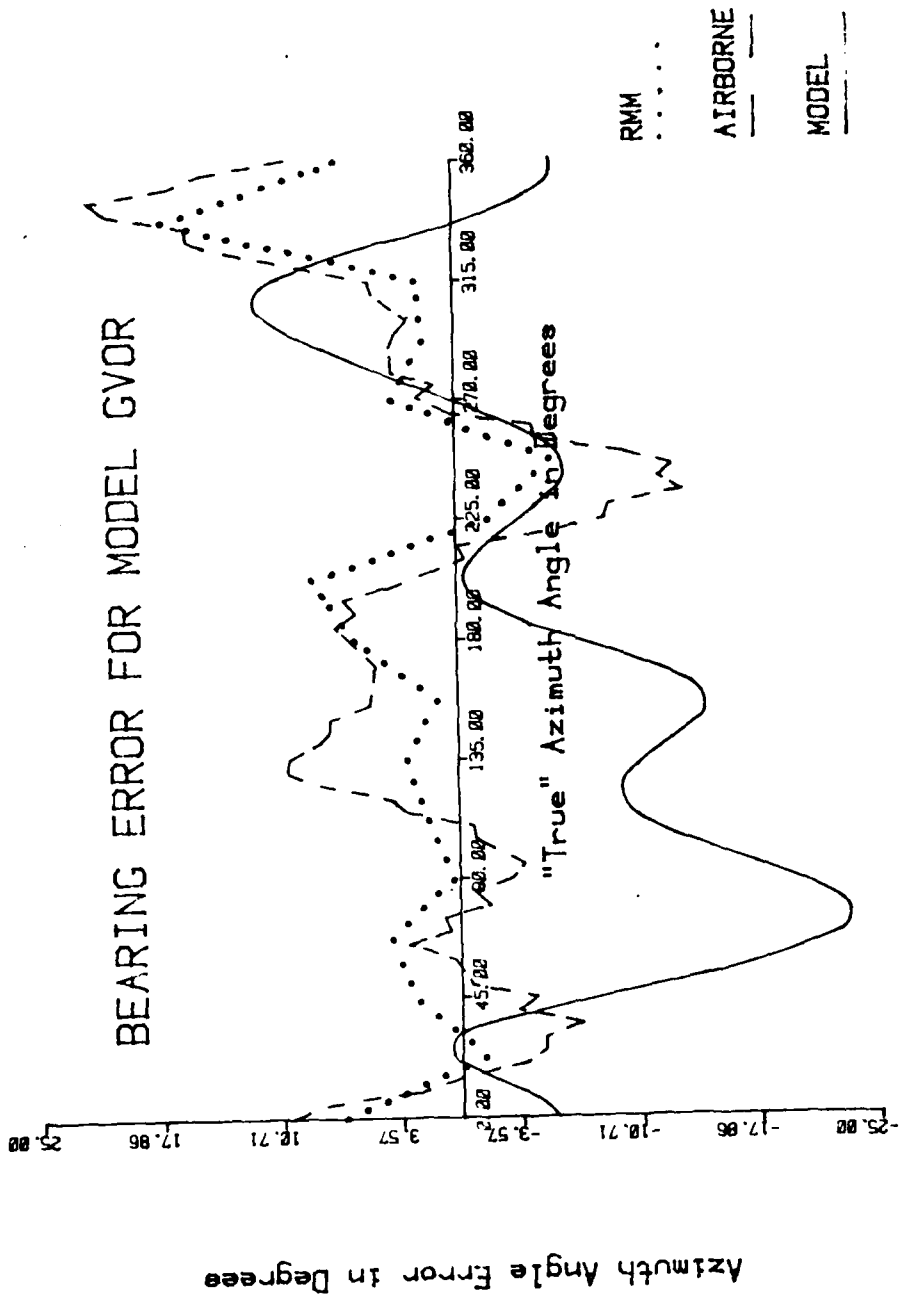


Figure 16 VOR errors due to parasitic scatterer No.(2): the scatterer was located on the 288 degree radial, mounted on the Radome, 48 inches above the counterpoise. The solid curve is model generated data. The dotted curve is data measured using the RMM system. The dashed curve represents data collected airborne, where  $R=6\text{Nmi.}$  and is the distance from the VOR system to the airplane.  $\text{Theta} = 82.94$  degrees.

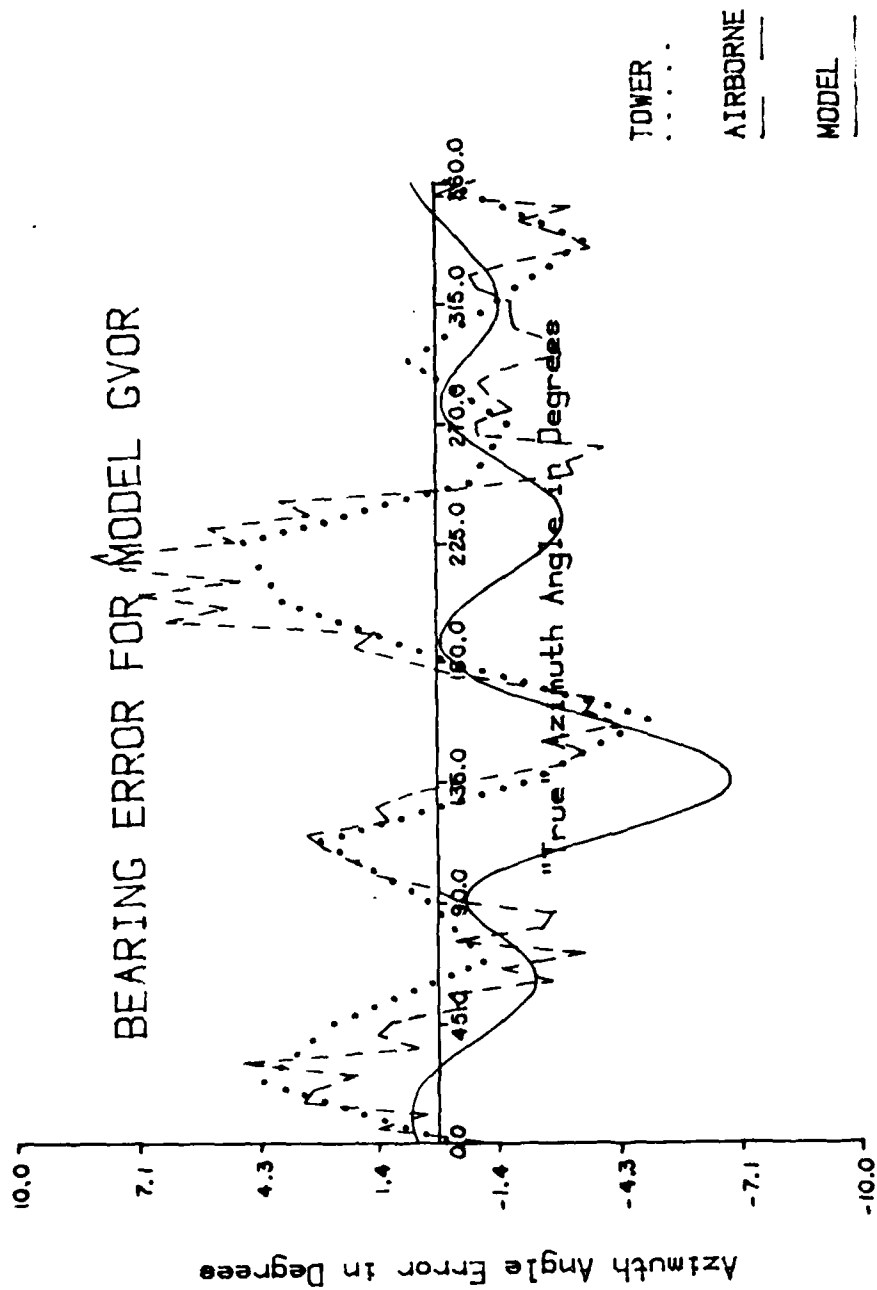


Figure 17 VOR errors due to parasitic scatterer No.(1): the scatterer was located on the 0 degree radial, mounted on the Radome, 72 inches above the counterpoise. The solid curve is model generated data. The dotted curve is data collected from a mobile tower, located 800 feet in radius from the VOR system. The dashed curve represents data collected airborne, where  $R=6\text{Nmi.}$  and is the distance from the VOR system to the airplane.  $\Theta = 82.94$  degrees.

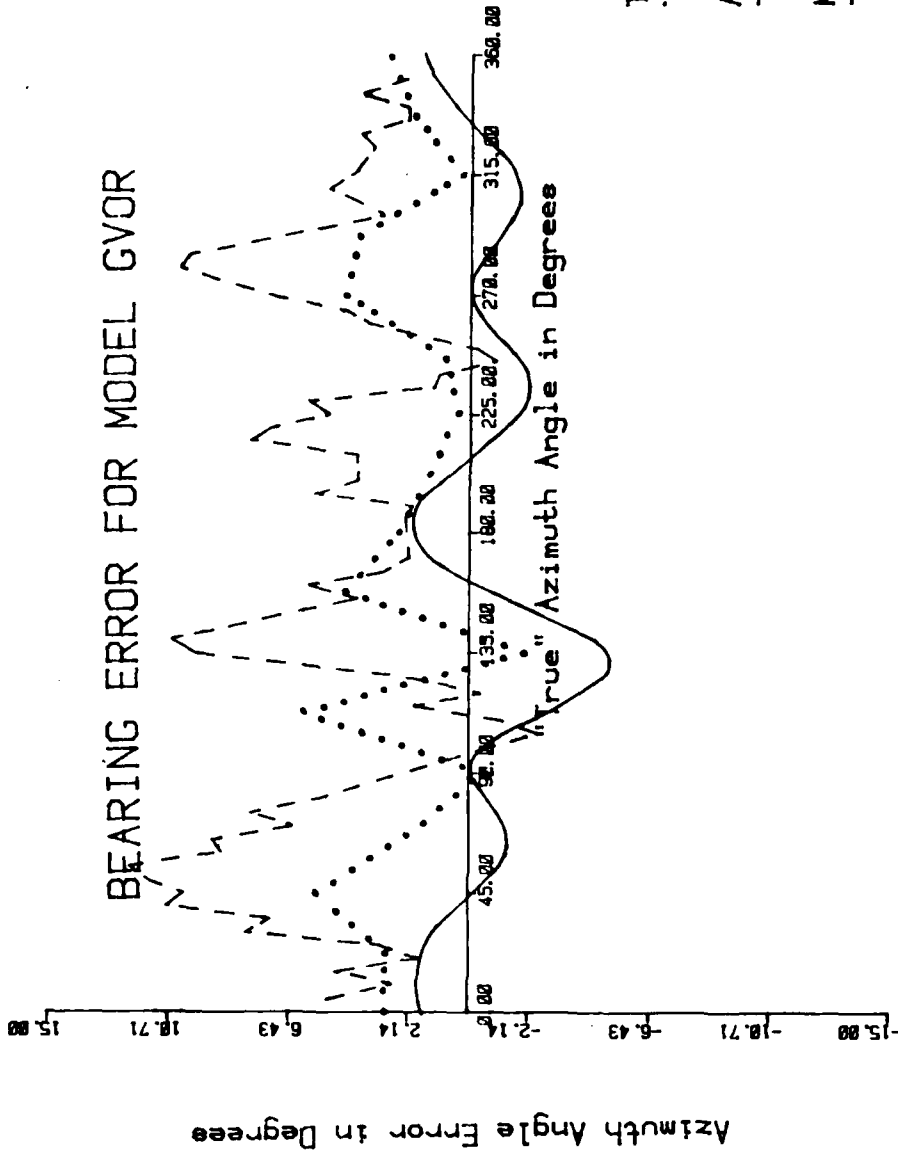


Figure 10 VOR errors due to parasitic scatterer No.(2): the scatterer was located on the 0 degree radial, mounted on the Radome, 24 inches above the counterpoise. The solid curve is model generated data. The dotted curve is data collected from a mobile tower, located 800 feet in radius from the VOR system. The dashed curve represents data collected airborne, where R=6Nmi. and is the distance from the VOR system to the airplane. Theta = 82.94 degrees.

# BEARING ERROR FOR MODEL GVOR

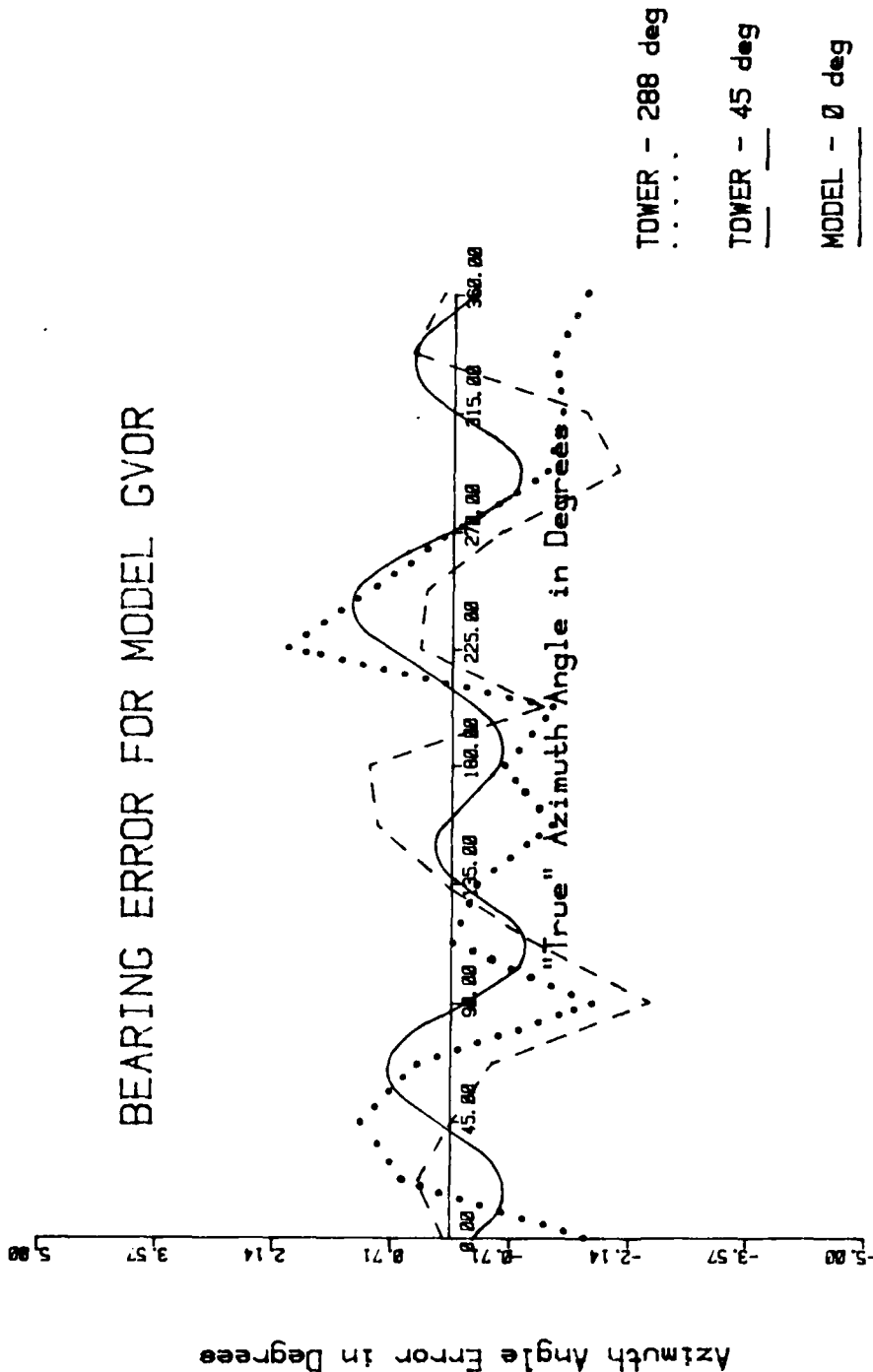


Figure 19 VOR errors due to parasitic scatterer No.(1): the scatterer was mounted on the Radome, 72 inches above the counterpoise. The solid curve is model generated data. The dotted curve represents data collected from a mobile tower, located 800 feet in radius from the VOR system. This dotted data was generated with the scatterer positioned on the 288 degree radial. The dashed curve also represents tower data, but with the scatterer lying on the 45 degree radial. The dotted and dashed curves have been phase-shifted to a reference of 0 degrees in radial.



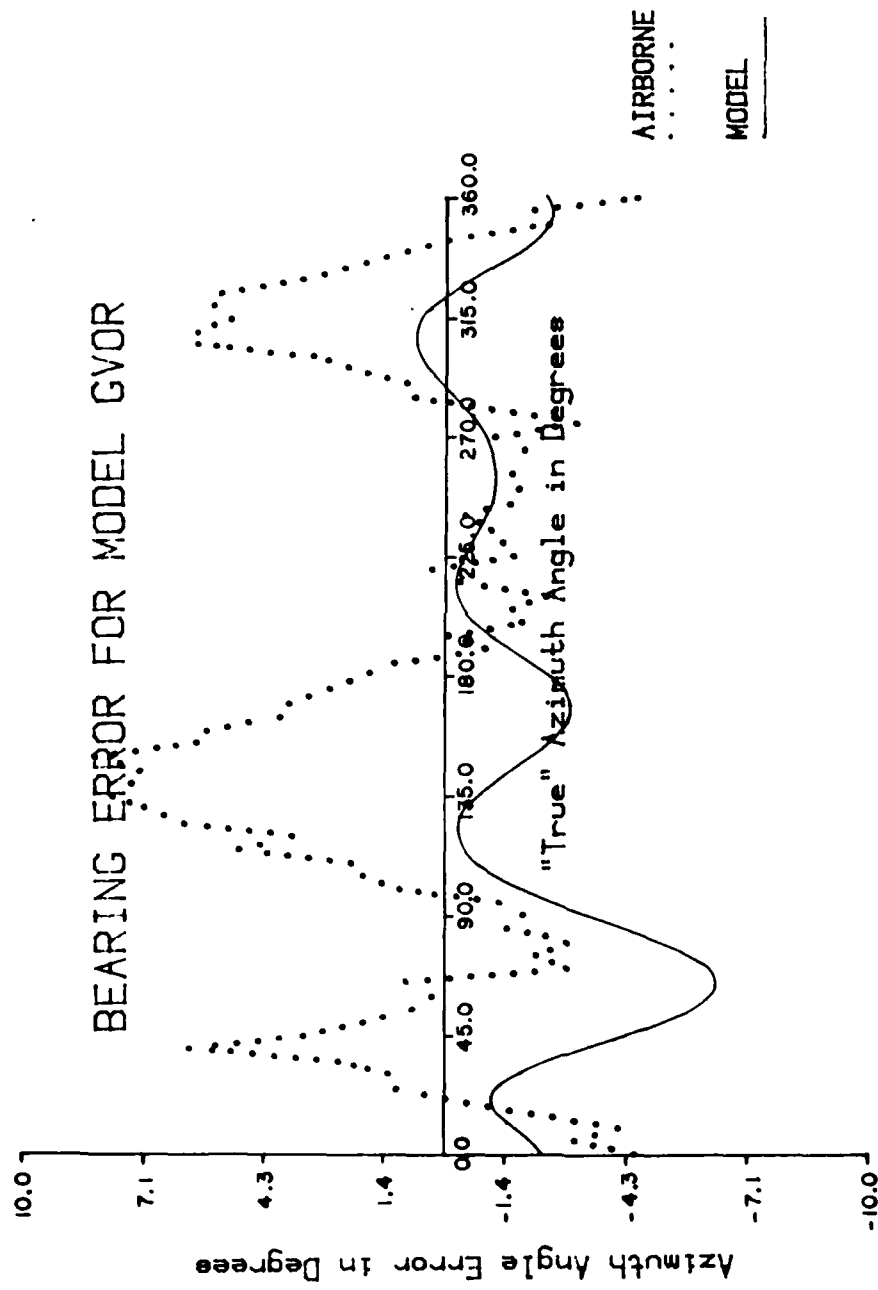


Figure 20 VOR errors due to parasitic scatterer No.(1): the scatterer was located on the 288 degree radial, mounted on the Radome, 72 inches above the counterpoise. The solid curve is model generated data. The dotted curve is airborne collected data, where R=6Nmi. and is the distance from the VOR system to the airplane. Theta = 82.94 degrees.

PEAK TO PEAK VOR ERROR					
FIG. #	CONFIG.	MODEL.	Rmm	TOWER	AIRBORNE
1	SCAT #1 45° 72" Hi	8.77	7.59	11.10	-----
2	SCAT #2 288° 48" Hi	35.33	22.99	-----	35.30
3	SCAT #1 0° 72" Hi	7.63	-----	9.70	12.70
4	SCAT #2 0° 24" Hi	7.03	-----	8.00	14.60
5	SCAT #1 228° 24" Hi	2.11	-----	3.70	-----
5	SCAT #1 45° 24" Hi	2.11	-----	3.40	-----
6	SCAT #1 288° 72" Hi	7.15	-----	-----	13.00

TABLE 2

they correlate well and other times they do not. This indicates that some error is present in the measured data. However, this error is not gross, and the measured data can confidently be used to get a general feeling for the shape of the error curve. And in all 6 figures, the modeled data displays the same general curvature as the measured data, indicating that model GVOR can account for the effects of horizontally polarized parasitic scatterers. It should be noted that when the measured data shows high correlation for a particular figure (using Table 2 and visual judgement on the figure), the modeled data also shows good agreement. But at this point a quantitative evaluation is not made due to the limited amount of measured data.

Figure 19 deserves some special attention. Although the two measured data sets were both collected from the far-field tower, one was with the scatterer positioned on the  $288^\circ$  radial, and the other was with the scatterer on the  $45^\circ$  degree radial. As indicated in the study for which the measured data were collected, the effect of rotating the scatterer around the radome "x" number of degrees was a phase shift in the error curve in the direction of rotation by "x" degrees. That is, if a data set was collected with the scatterer at  $0^\circ$  azimuth, and then a data set was collected with the scatterer at  $45^\circ$  azimuth, the two data sets would correlate highly when the latter set is phase shifted forward  $45^\circ$ . Therefore, the measured data in Figure 19 were confidently phase shifted to correspond to the scatterer being positioned at  $0^\circ$  azimuth, which is where the scatterer was located for the modeled data. It is worth mentioning that the modeled data also displayed the characteristic that

a rotation of scatterer position only resulted in the rotation of generated data.

### 3. Modeled results of vertically polarized parasitic scatterers

Vertically polarized parasitic scatterers were input to the VOR model, via NEC-2, in the form of straight wires placed perpendicular to the plane that holds the four VOR antennas. The results were identical to those obtained from the baseline model with no scatterers present. This was expected since GVOR completely ignores vertically polarized currents or fields. Recall that NTG , a GVOR subroutine, only reads in the horizontal components of electric field from NEC-2, so as to emulate the horizontally polarized VOR receiving antennas of aircraft.

#### IV. RECOMMENDATIONS

It is felt that the modeling approach used to create GVOR is valid due to the model's reasonable comparison against available measured data. However, for those interested in pursuing further development of this model, some suggestions are offered that may further enhance the results.

After the modeled results presented in previous sections were obtained, the model was modified to include the other three antennas as parasitic scatterers. In each of the modified program runs, one of the antennas is excited as usual, but all four antennas representing the VOR array are present. The goal is to account for any scattering effects neglected due to modeling the scatterer in the presence of only one antenna at a time. The appropriate modifications were made to the baseline model and to the scattering model. After both models were run, the output of the baseline model was subtracted from the output of the scattering model, leaving only the error due to scattering. This procedure, subtracting out the VOR baseline error, was performed on all the scattering data presented in this report.

Figures 21 and 22 illustrate the results obtained from the modified model, and correspond to the configurations used to obtain figures 15 and 18, respectively. It is evident that after the implementation of the above mentioned modifications the modeled data compares even more favorably with the measured data. However, after inspection of the

# BEARING ERROR FOR MODEL GVOR

Corresponds to Figure 15

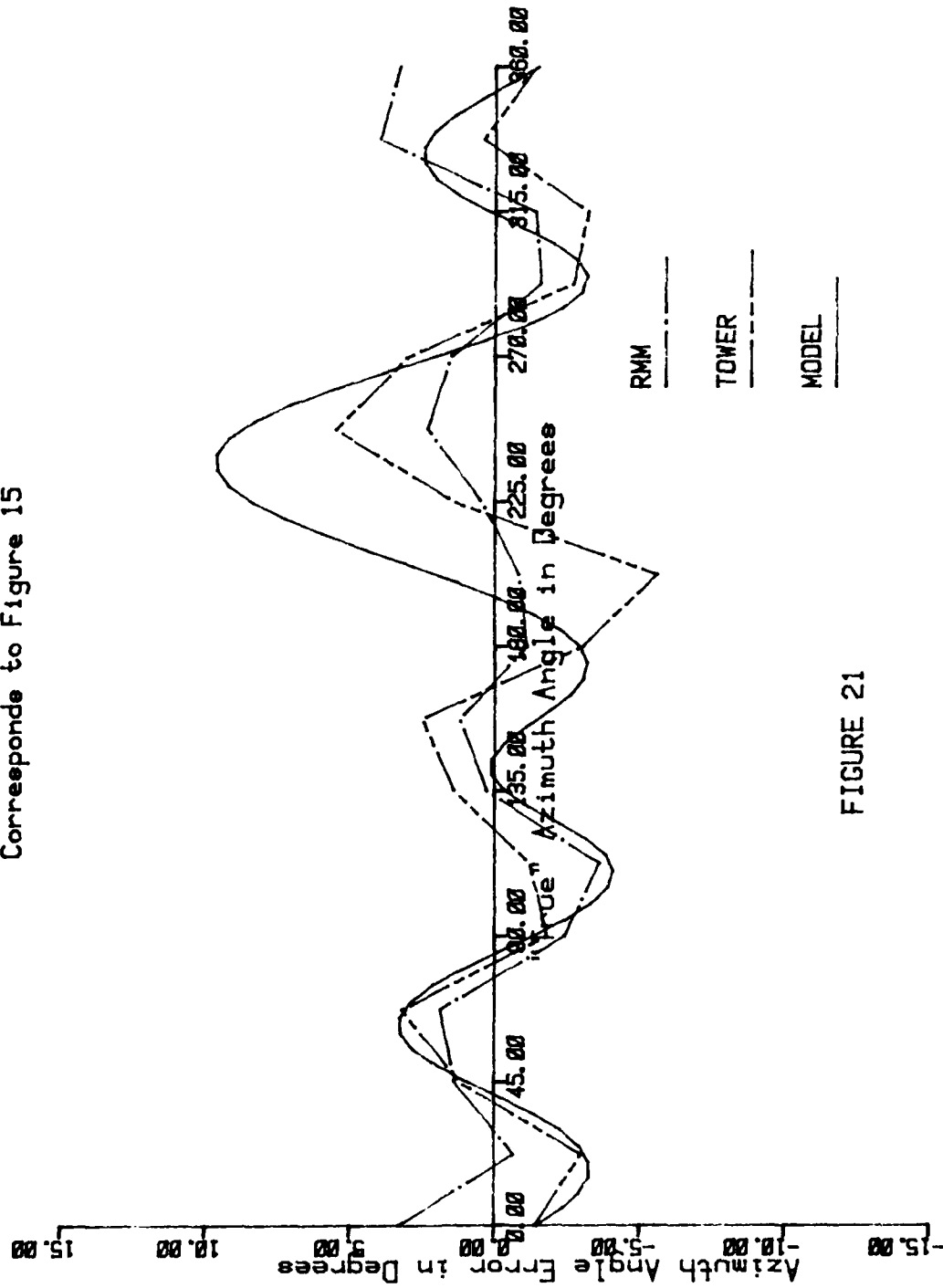


FIGURE 21

# BEARING ERROR FOR MODEL GVOR

Corresponds to Figure 18

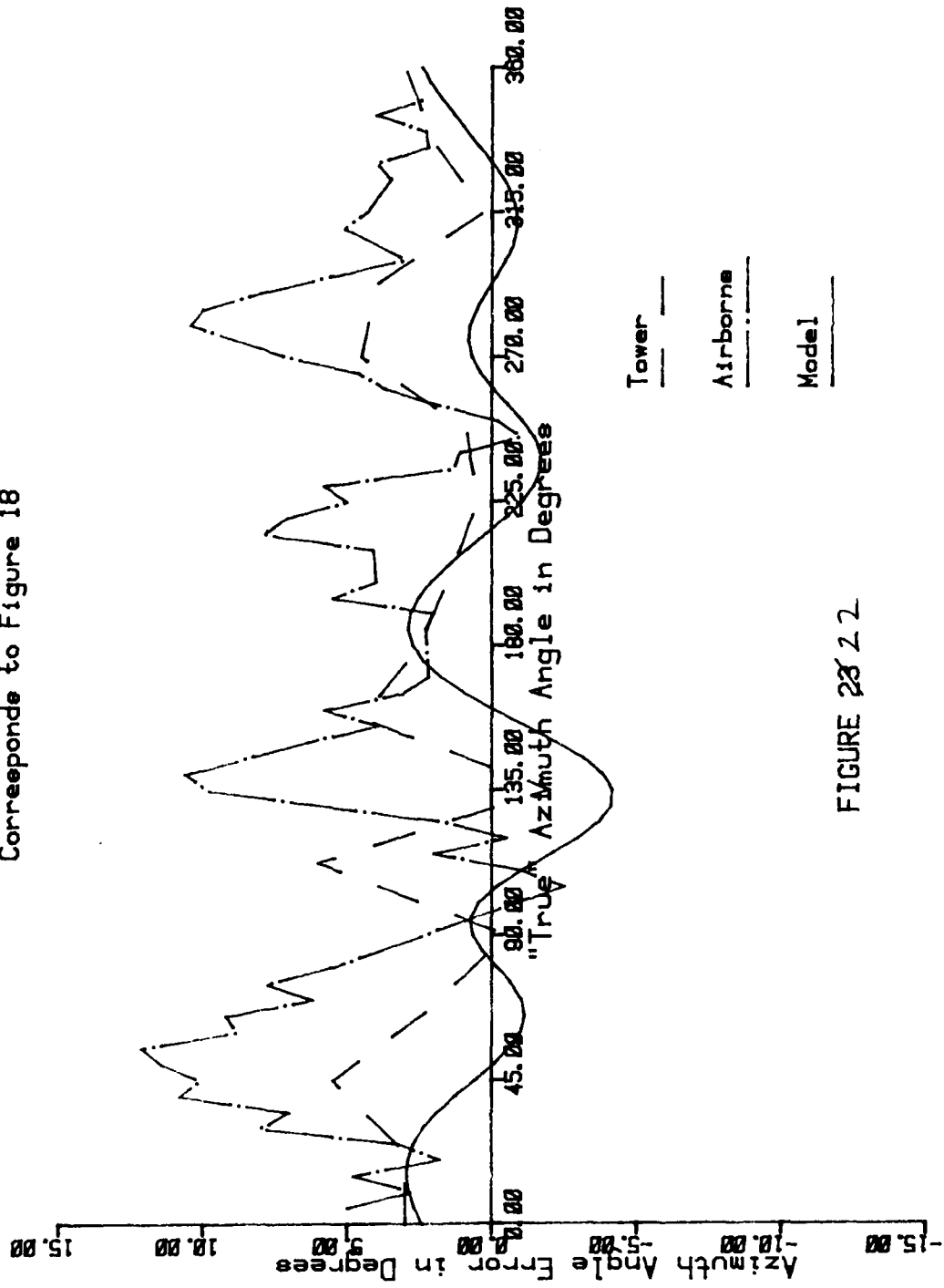


FIGURE 23 2 2

output from the baseline configuration (see Figure 23), it was decided not to present these modifications in the body of this report. The reason is that the author could not explain the negative bias displayed in this octantal error curve, especially after considering the highly symmetric nature of the VOR system. Additional work might be directed at finding a theoretical explanation for this phenomenon.

Also, for the further development of this model, it is recommended that the model be tested for several different scatterer configurations and then compared against measured data that represent these new configurations. It is emphasized that quality measured data are essential to any further model development. If good agreement is not found between the modeled and measured data, then other areas that may be looked into are:

1. Modification of the NEC.2 code so that a three dimensional model of the Alford Loop could be obtained.
2. Using NEC-2 to model the VOR counterpoise rather than proceeding with the infinite, perfectly conducting, ground plane approximation.
3. Incorporate the vertical field components output by NEC-2 into model GVOR, and adjust their magnitude in program GVOR to reflect a 30 dB. drop from that of the horizontal components, rather than neglecting the vertical field components all together.



# BEARING ERROR FOR MODEL GVOR

Baseline Output -- Dotantal Error Curve  
When 1 antenna is excited, other 3 are scatterers.

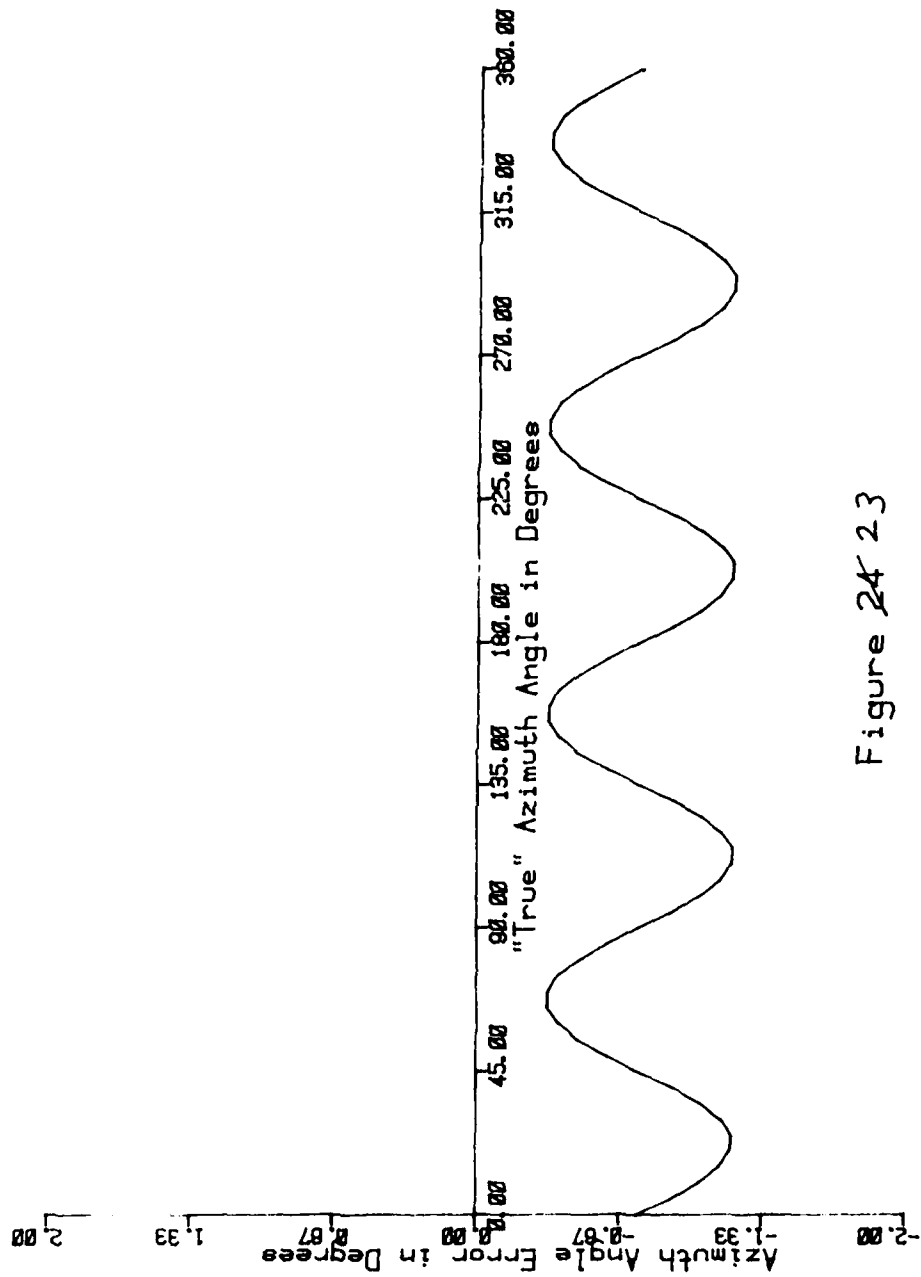


Figure 24 23

## V. ACKNOWLEDGEMENTS

The author wishes to thank Dr. Kent Chamberlin for his contributions as advisor and editor, and for the invaluable motivation he has provided. Also, acknowledgment is given to the Avionics Engineering Center of Ohio University for the access to its facilities.

## VI. REFERENCES

- [1] G. J. Burke and A. J. Poggio, *User's Guide to the Numerical Electromagnetics Code (NEC) - Method of Moments*, San Diego, California: Naval Ocean Systems Center, Technical Document 116, 3 vols., January 1981, vol. 1, pg. 1.
- [2] *1st Annual Review of Numerical Electromagnetics Code (NEC) Applications*, Livermore, Ca: Lawrence Livermore National Laboratory, Proceedings, March 1985.
- [3] F. J. Doadrick, G. J. Burke, and A. J. Poggio, *Computer Analysis of the Trussed-Whip and Discone-Cage Antennas*, Livermore, Ca: Lawrence Livermore National Laboratory, report, January 1977.
- [4] Allen W. Glisson and Donald R. Wilton, *Numerical Procedures for Handling Stepped-Radius Wire Junctions*, San Diego, Ca: Naval Ocean Systems Center, report, March 1979.
- [5] Jerry Burke, Telephone conversation focusing on successful applications of NEC-2, Livermore, Ca: Lawrence Livermore National Laboratory, personal communication, 4 PM EST, October 23, 1985.
- [6] Jeff Dennis and Robert Redlich, *Assessment of Correlation Between Second Generation VOR Monitoring and the VOR Signal in Space*, Athens, OH: Ohio University Avionics Engineering Center, Technical Report EER-74-1, March 1985.
- [7] Federal Aviation Administration, *Very High Frequency Omnitrange*, Oklahoma City, Oklahoma: FAA Aeronautical Center, Manual FV-201-1, October 1969, Ch. 1, pg. 1.
- [8] *Ibid*, Ch. 1, pg. 1-3.
- [9] *Ibid*, Ch. 3, pg. 16-19.
- [10] *Ibid*, Ch. 1, pg. 3.
- [11] *Ibid*, Ch. 1, pg. 3.
- [12] *Ibid*, Ch. 1, pg. 4.
- [13] *Ibid*, Ch. 1, pg. 1-3.
- [14] *Ibid*, Ch. 7, pg. 21-24.
- [15] *Ibid*, Ch. 1, pg. 10.
- [16] *Ibid*, Ch. 3, pg. 9-25.

- [17] Alan V. Oppenheim and Ronald W. Schaffer, *Digital Signal Processing*, Englewood Cliffs, New Jersey: Prentice-Hall, Inc., 1975, Ch. 6, pg. 290-294.
- [18] Wai-Kai Chen, *Linear Networks and Systems*, Monterey, California: Brooks/Cole Engineering Division, 1983, Ch. 8, pg. 325-333.
- [19] Alan V. Oppenheim and Ronald W. Schaffer, *op. cit.*, pg. 290-299.
- [20] Federal Aviation Administration, *op. cit.*, Ch. 2, pg. 5, Ch. 3, pg. 23.
- [21] G. J. Burke and A. J. Poggio, *op. cit.*, vol. 1, pg. 9-31.
- [22] G. J. Burke and A. J. Poggio, *op. cit.*, vol. 2, pg. 1.
- [23] G. J. Burke and A. J. Poggio, *op. cit.*, vol. 1, pg. 75-78.
- [24] G. J. Burke and A. J. Poggio, *op. cit.*, vol. 2, pg. 14-89.
- [25] G. J. Burke and A. J. Poggio, *op. cit.*, vol. 1, pg. 1.
- [26] G. J. Burke and A. J. Poggio, *op. cit.*, vol. 2, pg. 1.
- [27] G. J. Burke and A. J. Poggio, *op. cit.*, vol. 2, pg. 6-11.
- [28] G. J. Burke and A. J. Poggio, *op. cit.*, vol. 2, pg. 3-6.
- [29] Federal Aviation Administration, *op. cit.*, Ch. 7, pg. 19-21.
- [30] Constantine A. Balanis, *Antenna Theory - Analysis and Design*, New York, NY: Harper & Row, Publishers, Inc., 1982, Ch. 5.
- [31] F. J. Deadrick, G. J. Burke, and A. J. Poggio, *Computer Analysis of the Trussed-Whip and Discone-Cage Antennas*, Livermore, Ca: Lawrence Livermore National Laboratory, report, January 1977.
- [32] Jerry Burke, Telephone conversation focusing on successful applications of NEC-2, Livermore, Ca: Lawrence Livermore National Laboratory, personal communication, 4 PM EST, October 23, 1985.
- [33] Constantine A. Balanis, *op. cit.*, Ch. 5., pg. 181.
- [34] G. J. Burke and A. J. Poggio, *op. cit.*, vol. 2, pg. 7-8.
- [35] G. J. Burke and A. J. Poggio, *op. cit.*, vol. 2, pg. 3,8.
- [36] Federal Aviation Administration, *op. cit.*, Ch. 7, pg. 57.
- [37] George Sakai, Telephone conversation, Washington, D.C.: Federal Aviation Administration, personal communication, May 8, 1985.

- [38] Federal Aviation Administration, *op. cit.*, Ch. 2, pg. 5.
- [39] Federal Aviation Administration, *op. cit.*, Ch. 7, pg. 25-31.
- [40] Jeff Dennis and Robert Redlich, *Assessment of Correlation Between Second Generation VOR Monitoring and the VOR Signal in Space*, Athens, OH: Ohio University Avionics Engineering Center, Technical Report EER-74-1, March 1985.

## VII. APPENDICES

A. Algorithm for Calculating the Received Time-Domain VOR Signal

B. Code Listings

1. KCVOR (circular radiation patterns from transmitting antennas)

2. KCVOR-M (modified to simulate elliptical radiation patterns)

3. GVOR

4. NECIN.DAT (NEC-2 input for baseline VOR -- no scatterers)

5. NECSCIN.DAT (NEC-2 input for VOR + scatterer configuration)

C. User's Section

## APPENDIX A

Algorithm for Calculating the Received Time-Domain VOR Signal

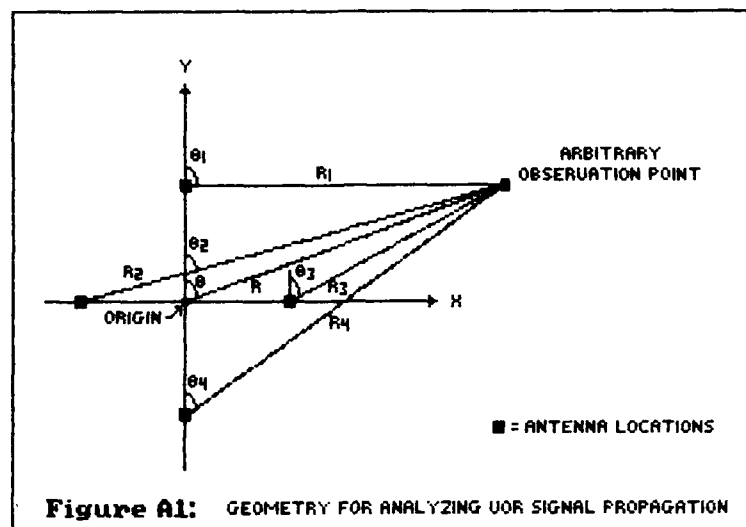


Figure A1 shows a geometry that can be used to determine the composite field radiated by the VOR at an arbitrary observation point. To calculate the phase of the field from antenna "n", the following equation is used:

$$\text{phase}_n = e^{-j\beta R_n} \quad (\text{A.1})$$

where "n" is the antenna number, beta is the phase constant, and  $R_n$  is the distance between the antenna to the observation point. The distance between the phase center and the observation point is  $R$ , as shown in Figure A1.

A far-field approximation is eventually assumed so that the  $1/R$  field-strength-terms for each of the four signals can be considered equal, and so the navigational data is contained in the phase terms of these signals. For this reason, the antenna fields are represented by their phase terms only.



The received field due to the VOR variable signal is given by:

$$\mathbf{CREC} = \mathbf{CREF} + [\mathbf{CP1} * \sin \omega t] + [\mathbf{CP2} * \cos \omega t] \quad (\text{A.2})$$

where CREC is the complex-valued received field, CREF is the reference signal, CP1 is the signal from antenna pair #1, and CP2 is the signal from antenna pair #2. The sine and cosine terms account for the 90° phase difference between the two goniometer output lines as discussed in section B-1 of *Model Development*. These two terms when added together form the VOR composite sideband (see Figure A2). The composite sideband has a figure-eight radiation pattern which rotates in azimuth at 30 revolutions per second, and which, when added to CREF, results in a limaçon radiation pattern (see Figure A3) about the VOR that also rotates at 30 revolutions per second.

Using equation (A.1), equation (A.2) can be expanded as follows:

$$\mathbf{CREF} = \sum_{i=1}^N e^{-j\beta R_i}$$

$$\mathbf{CP1} = (e^{-j\beta R_1} - e^{-j\beta R_4})$$

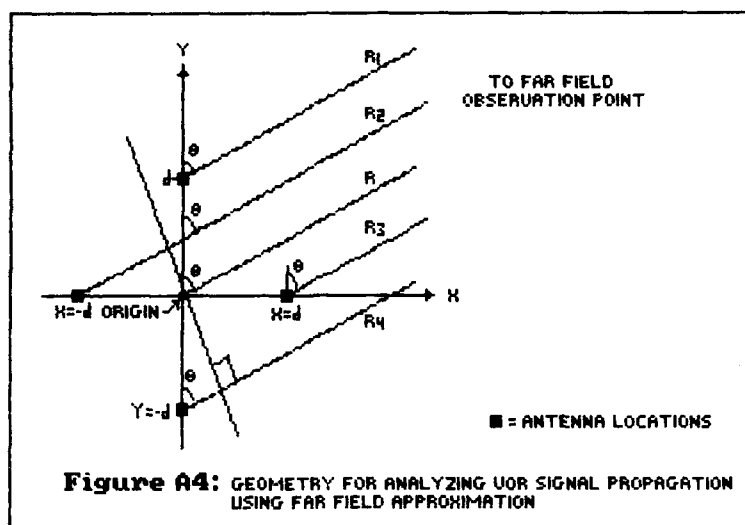
$$\mathbf{CP2} = (e^{-j\beta R_3} - e^{-j\beta R_2})$$

so that

$$\begin{aligned} \mathbf{CREC} = & \sum_{i=1}^N e^{-j\beta R_i} + (e^{-j\beta R_1} - e^{-j\beta R_4}) \sin \omega t \\ & + (e^{-j\beta R_3} - e^{-j\beta R_2}) \cos \omega t \end{aligned}$$

or, re-writing:

$$\begin{aligned} \mathbf{CREC} = & e^{-j\beta R_1} (1 + \sin \omega t) + e^{-j\beta R_2} (1 - \cos \omega t) \\ & + e^{-j\beta R_3} (1 + \cos \omega t) + e^{-j\beta R_4} (1 - \sin \omega t) \end{aligned}$$



Assuming far field observations, Figure A1 can be approximated by Figure A4. By applying basic trigonometry to Figure A4, it can be shown that:

$$\begin{aligned}
 R_2 &= R + d * \sin \theta \\
 R_3 &= R - d * \sin \theta \\
 R_1 &= R - d * \cos \theta \\
 R_4 &= R + d * \cos \theta
 \end{aligned}
 \tag{A.3.1-4}$$

Equations (A.3.1-4) can be rewritten as:

$$\begin{aligned}
 R_2 &= R + R_b = R + d * \sin \theta \\
 R_3 &= R - R_c = R - d * \sin \theta \\
 R_1 &= R - R_3 = R - d * \cos \theta \\
 R_4 &= R + R_d = R + d * \cos \theta
 \end{aligned}
 \tag{A.4.1-4}$$

where  $R_a$  through  $R_d$  represent the "normalized" ranges for antennas 1 through 4, respectively.

Substituting equations (A.4.1-4) into the last equation for CREC, the following are obtained:

$$\begin{aligned} \text{CREC} &= e^{-j\beta(R+R_a)}(1 + \sin \omega t) \\ &+ e^{-j\beta(R+R_b)}(1 - \cos \omega t) \\ &+ e^{-j\beta(R+R_c)}(1 + \cos \omega t) \\ &+ e^{-j\beta(R+R_d)}(1 - \sin \omega t) \end{aligned}$$

$$\text{CREC} = \left\{ e^{-j\beta R_a}(1 + \sin \omega t) + e^{-j\beta R_b}(1 - \cos \omega t) + e^{-j\beta R_c}(1 + \cos \omega t) + e^{-j\beta R_d}(1 - \sin \omega t) \right\} e^{-j\beta R} \quad (\text{A.5})$$

Note that if  $R$  is subtracted from  $R_n$ , where  $n$  equals 1 through 4, before CREC is calculated, the result would be:

$$\begin{aligned} R_1 - R &= R_a & R_3 - R &= R_c \\ R_2 - R &= R_b & R_4 - R &= R_d \end{aligned}$$

$$\text{CREC} = e^{-j\beta R_a}(1 + \sin \omega t) + e^{-j\beta R_b}(1 - \cos \omega t) + e^{-j\beta R_c}(1 + \cos \omega t) + e^{-j\beta R_d}(1 - \sin \omega t) \quad (\text{A.6})$$

Comparing equations (A.5) and (A.6), it becomes evident that the process of "normalizing" the range vectors is equivalent to setting  $R=0$  in equation (A.5).

Note that  $R \gg R_a, R_b, R_c, R_d$ . By normalizing the range vectors, the constant phase shift introduced by the  $e^{-j\beta R}$  term is set to 0 degrees

(exactly), independent of the value of  $R$  used. Therefore, by normalizing the range values, errors due to computing complex exponentials with large arguments are reduced significantly.

Appendix B  
Code Listings

C \*\*\* PROGRAM KCVOR \*\*\*

C Paul R. Barré

C 1 JUNE 1986

C THIS PROGRAM MODELS THE VOR NAVIGATION SYSTEM

C THE AZIMUTH IS INCREMENTED IN 5-DEGREE STEPS FROM 0  
C TO 360 DEGREES. FOR A GIVEN AZIMUTH ANGLE, TIME IS  
C INCREMENTED FROM 0 TO 1/30 SECONDS IN 256 STEPS.

C A FAST FOURIER TRANSFORM IS USED TO DETERMINE THE PHASE  
C OF THE RECEIVED 30 HZ SIGNAL. THE ERROR IS THEN CALCULATED  
C USING THE DIFFERENCE BETWEEN THE AZIMUTH AND THE PHASE OF  
C THE 30 HZ SIGNAL.

C MMPLOT IS THEN USED TO PLOT ERROR VS. AZIMTUH

C THIS VERSION USES A DOUBLE PRECISION FFT ROUTINE

C THE FFT ROUTINE(DPFFT) MUST BE PASSED THE REAL AND  
C IMAGINARY COMPONENT ARRAYS AND THE NUMBER OF DATA  
C POINTS AS A POWER OF 2 (I.E. FOR 256 DATA POINTS, 8 IS  
C PASSED TO THE FFT ROUTINE, 256=2\*\*8).

C  
C IMPLICIT COMPLEX\*16 (C)  
C IMPLICIT REAL\*8 (A,B,D-H,O-Y)  
C DIMENSION XR(256),XI(256)  
C DIMENSION C(4),XA(4),YA(4),RA(4),CE(4)  
C DIMENSION ZXP(73),ZYP(73)

C SET CONSTANTS

C  
C DATA VC/3.DB/,FREQ/115.D6/,D/0.656D0/,R/5000.D0/  
C DATA XA/0.D0,-.199D0,.199D0,0.D0/,YA/.199D0,0.D0,0.D0,-.199D0/  
C PI = DARCOS(-1.D0)  
C BETA = (2.D0\*PI\*FREQ)/VC  
C OMEGAM = 2.D0\*PI\*30.D0

C OUTSIDE LOOP INCREMENTS AZIMUTH ANGLE IN 5 DEGREE STEPS

C  
C DO 30 IAZ = 1,73  
C AZ = DFLOAT(IAZ-1)\*5.D0  
C AZR = AZ \* PI/180.D0

C FIND X,Y COORDINATES

C  
C X = R\*DSIN(AZR)  
C Y = R\*DCOS(AZR)

```

C      THIS LOOP CALCULATES THE NORMALIZED DISTANCE (RA) FROM EACH ARRAY
C      ELEMENT TO THE OBSERVATION POINT.
C
DO 10 I = 1,4
RA(I) = DSQRT((X-XA(I))**2+(Y-YA(I))**2) - R
C(I) = DCMPLX(0.D0,-BETA*RA(I))
CE(I)=CDEXP(C(I))
10 CONTINUE
C
C      FORM RADIATING PAIRS
C
CP1 = CE(1) - CE(4)
CP2 = CE(3) - CE(2)
C
C      CYCLE TIME FROM 0 TO 1/30 SECONDS IN 256 STEPS
C
DO 20 INC = 1,256
T = DFLOAT(INC-1)/(256.D0*30.D0)
CREF = DCMPLX(0.D0,2.D0)
C
C      CALCULATE RECEIVED FIELD FOR GIVEN TIME AND POSITION
C
CREC(INC) = CREF + CP1*DSIN(OMEGAM*T) + CP2*DCOS(OMEGAM*T)
XR(INC) = DREAL(CREC(INC))
XI(INC) = DIMAG(CREC(INC))
20 CONTINUE
C
C      CALL FAST FOURIER TRANSFORM ROUTINE
C
CALL DPFFT(XR,XI,8)
C
C      LOOK THE 30 HERTZ COMPONENT AND DETERMINE THE PHASE AND MAGNITUDE
C
NI = 2
VAZ = DATAN2(XI(NI),XR(NI))*(180.D0/PI)
C
C      ADJUST PHASE SO ALL VALUES ARE BETWEEN 0 AND 360 DEGREES
C
IF(VAZ.LT.0.D0) VAZ = VAZ + 360.D0
C
C      CALCULATE ERROR BETWEEN AZIMUTH ANGLE AND RECEIVED PHASE
C
ERROR = AZ - VAZ
ZXP(IAZ)=AZ
ZYP(IAZ)=ERROR
PRINT 2, AZ,VAZ,ERROR
2  FORMAT(1X,3F15.5)
30 CONTINUE
CALL MMPLLOT(ZXP,ZYP,73,1,ZXLAB,ZYLAB)
STOP
END

```

```

C
C
      SUBROUTINE DPFFT(FR,FI,K)
      IMPLICIT REAL*8 (A-H,O-Z)
C - FAST FOURIER TRANSFORM USING TIME DECOMPOSITION
C - DATA IS IN FR (REAL) AND FI (IMAGINARY) ARRAYS.
C - COMPUTATION IS IN PLACE, OUTPUT REPLACES INPUT
C - NUMBER OF POINTS MUST BE 2**K
C - FR(N) AND FI(N) MUST BE DIMENSIONED IN MAIN PROGRAM
      DIMENSION FR(1),FI(1)
      N=2**K
      MR=0
      NN=N-1
      DO 2 M=1,NN
      L=N
1  L=L/2
      IF(MR+L.GT.NN) GO TO 1
      MR=MOD(MR,L)+L
      IF (MR.LE.M) GO TO 2
      TR=FR(M+1)
      FR(M+1)=FR(MR+1)
      FR(MR+1)=TR
      TI=FI(M+1)
      FI(M+1)=FI(MR+1)
      FI(MR+1)=TI
2  CONTINUE
      L=1
3  IF(L.GE.N) RETURN
      ISTEP=2*L
      EL=L
      DO 4 M=1,L
      A=DARCOS(-1.D0)*DFLOAT(1-M)/EL
      WR=DCOS(A)
      WI=DSIN(A)
      DO 4 I=M,N,ISTEP
      J=I+L
      TR=WR*FR(J)-WI*FI(J)
      TI=WR*FI(J)+WI*FR(J)
      FR(J)=FR(I)-TR
      FI(J)=FI(I)-TI
      FR(I)=FR(I)+TR
4  FI(I)=FI(I)+TI
      L=ISTEP
      GO TO 3
      END

```



\*\*\* PROGRAM KCVOR-M \*\*\*

Paul R. Barré  
1 JUNE 1986

THIS PROGRAM MODELS AN IDEAL VOR NAVIGATION SYSTEM AND SIMULATES ALFORD LOOP ANTENNA END PLATE ADJUSTMENTS FOR REDUCTION OF OCTANTAL ERROR.

THE AZIMUTH IS INCREMENTED IN 5-DEGREE STEPS FROM 0 TO 360 DEGREES (73 times). FOR A GIVEN AZIMUTH ANGLE, TIME IS INCREMENTED FROM 0 TO 1/30 SECONDS IN 256 STEPS IN ORDER TO SIMULATE RECEIVING A FULL PERIOD OF SIGNAL WITH APPROPRIATE RESOLUTION.

A FAST FOURIER TRANSFORM IS USED TO DETERMINE THE PHASE OF THE RECEIVED 30 HZ SIGNAL. THE ERROR IS THEN CALCULATED USING THE DIFFERENCE BETWEEN THE AZIMUTH AND THE PHASE OF THE 30 HZ SIGNAL.

MMPLOT IS THEN USED TO PLOT ERROR VS. AZIMTUH

THIS VERSION USES A DOUBLE PRECISION FFT ROUTINE

THE FFT ROUTINE(DPFFT) MUST BE PASSED THE REAL AND IMAGINARY COMPONENT ARRAYS AND THE NUMBER OF DATA POINTS AS A POWER OF 2 (I.E. FOR 256 DATA POINTS, 8 IS PASSED TO THE FFT ROUTINE,  $256=2^{**8}$ ).

IMPLICIT COMPLEX (C)  
IMPLICIT REAL\*8 (A,B,D-H,O-Y)  
IMPLICIT LOGICAL(F)  
COMPLEX CREC, CE, C  
DIMENSION XR(256),XI(256),CREC(256)  
DIMENSION ZXP(73),ZYP(73),XA(4),YA(4),RA(4),CE(4),C(4)

SET CONSTANTS

DATA VC/3.D8/,RFREQ/115.D6/,D/0.656D0/,R/5000.D0/  
DATA XA/0.D0,-.199D0,.199D0,0.D0/,YA/.199D0,0.D0,0.D0,-.199D0/  
PI = DACOS(-1.D0)  
BETA = (2.D0\*PI\*RFREQ)/VC  
OMEGAM = 2.D0\*PI\*30.D0

OUTSIDE LOOP USED TO ZERO IN ON OPTIMUM "ELLIPSE" FACTOR

DO 91 L=1,11  
A=0.9608D0+FLOAT(L-1)\*0.00008D0  
B=2.D0-A  
DO 30 IAZ = 1,73

```

AZ = FLOAT(IAZ-1)*5.DO
AZR = AZ * PI/180.DO

C
C
C      FIND X,Y COORDINATES AND CALCULATE "ELLIPSE" FACTOR
C
X = R*DSIN(AZR)
Y = R*DCOS(AZR)
AEF = 1.DO / DSQRT( A*DCOS(AZR)**2 + B*DSIN(AZR)**2 )
BEF = 1.DO / DSQRT( B*DCOS(AZR)**2 + A*DSIN(AZR)**2 )

C
C      THIS LOOP CALCULATES THE DISTANCE(R) FROM EACH ARRAY
C      ELEMENT TO THE OBSERVATION POINT
C
DO 10 I = 1,4
  RA(I) = DSQRT((X-XA(I))**2+(Y-YA(I))**2) - R
  C(I) = CMLPX(0.DO,-BETA*RA(I))
  CTEMP = C(I)
  IF(I.EQ.1) CE(I) = CEXP(CTEMP) * AEF
  IF(I.EQ.2) CE(I) = BEF * CEXP(CTEMP)
  IF(I.EQ.3) CE(I) = BEF * CEXP(CTEMP)
  IF(I.EQ.4) CE(I) = CEXP(CTEMP) * AEF
10 CONTINUE
CP1 = CE(1) - CE(4)
CP2 = CE(3) - CE(2)

C
C      CYCLE TIME FROM 0 TO 1/30 SECONDS IN 256 STEPS
C
DO 20 INC = 1,256
  T = FLOAT(INC-1)/(256.DO*30.DO)
  CBIAS = CMLPX(0.DO,2.DO)

C
C      CALCULATE RECEIVED FIELD FOR GIVEN TIME AND POSITION
C
CREC(INC) = CBIAS + CP1*DSIN(OMEGAM*T) + CP2*DCOS(OMEGAM*T)
CTEMP = CREC(INC)
XR(INC) = REAL(CTEMP)
XI(INC) = AIMAG(CTEMP)
20 CONTINUE

C
C      CALL FAST FOURIER TRANSFORM ROUTINE
C
CALL PDFFTB(XR,XI,8)

C
C      LOOK THE 30 HERTZ COMPONENT AND DETERMINE THE PHASE AND MAGNITUDE
C
NI = 2
FREALZ=.FALSE.
FIMAGZ=.FALSE.
VAZ=DATAN2(XI(NI),XR(NI))*(180.0/PI)
IF((XI(NI).LT.1.E-4).AND.(XI(NI).GT.-1.E-4)) THEN
  VAZ=-180.

```

```
      IF(XR(NI).GT.0.0) VAZ=0.0
      FIMAGZ=.TRUE.
    END IF
    IF((XR(NI).LT.1.E-4).AND.(XR(NI).GT.-1.E-4)) THEN
      VAZ=-90.
      IF(XI(NI).GT.0.0) VAZ=90.
      FREALZ=.TRUE.
    END IF
    IF((FREALZ).AND.(FIMAGZ)) THEN
      VAZ=99999999.
      WRITE(*,103)
      FORMAT(/1X,'NO SIGNAL RECEIVED')
    END IF
103
C
C   ADJUST PHASE SO ALL VALUES ARE BEWTEEN 0 AND 360 DEGREES
C
      IF(VAZ.LT.0.D0) VAZ = VAZ + 360.D0
C
C   CALCULATE ERROR BETWEEN AZIMUTH ANGLE AND RECEIVED PHASE
C
      ERROR = AZ - VAZ
      ZXP(IAZ)=AZ
      ZYP(IAZ)=ERROR
      PRINT 2, AZ,VAZ,ERROR
      FORMAT(1X,3F15.5)
2
30   CONTINUE
C   CALL MMPLLOT(ZXP,ZYP,73,1,ZXLAB,ZYLAB)
91   CONTINUE
      STOP
      END
```



```

C      T = CORRESPONDS TO TIME
C      VAZD = VOR SYSTEM PHASE OUTPUT IN DEGREES
C      VLTSPM = MAGNITUDE OF FAR FIELD VOLTAGE (1 of 4, generated by NEC)
C      XI = IMAGINARY PART OF VARIABLE SIGNAL (rotating cardioid)
C      XR = REAL PART OF VARIABLE SIGNAL (rotating cardioid)
C
CCCCCCCCCCCCCCCCCCCCCCCCCCCCCCCCCCCCCCCCCCCCCCCCCCCCCCCCCCCCCCCCCCCCCCCC
C
      IMPLICIT COMPLEX*16 (C)
      IMPLICIT REAL*8 (A,B,D-H,O-Y)
      DIMENSION XVR(256),XVI(256)
      DIMENSION CE(4)
      DIMENSION PHI(73,4),VLTSPM(73,4),FAZD(73,4),AZN(73)
      DIMENSION RLVLTG(73,4),AIMVLT(73,4)

C
C      SET CONSTANTS
C
      PI = DACOS(-1.D0)
      OMEGAM = 2.D0*PI*30.D0

C
C      GET INPUT DATA FROM NEC AND PUT INTO USABLE FORM
C
      CALL NTG(PHI,VLTSPM,FAZD)
      DO 55 I=1,73
        AZN(I) = PHI(I,1)
        DO 55 N=1,4
          FAZR=FAZD(I,N)*PI/180.D0
          RLVLTG(I,N)=VLTSPM(I,N)*DCOS(FAZR)
          AIMVLT(I,N)=VLTSPM(I,N)*DSIN(FAZR)
55      CONTINUE

C
C      OUTSIDE LOOP INCREMENTS AZIMUTH ANGLE IN 5 DEGREE STEPS
C
      DO 30 IAZ = 1,73
        AZ = DFLOAT(IAZ-1)*5.D0
        AZR = AZ * PI/180.D0
        AZRN=AZN(IAZ) * PI/180.D0
        IF(AZR.NE.AZRN) THEN
          WRITE(6,112)
112      FORMAT(1X,'AZIMUTH ANGLE FROM NEC DOES NOT MATCH GVOR AZIMUTH')
          STOP
        END IF

C
C      THIS LOOP CALCULATES THE COMPLEX E-FIELD AT THE OBSERVATION
C      POINT AND ALSO DETERMINES IT'S PHASE
C
      DO 10 I = 1,4
        CE(I)=DCMLX(RLVLTG(IAZ,I),AIMVLT(IAZ,I))
10      CONTINUE
C

```

```

CP1 = CE(1) - CE(4)
CP2 = CE(3) - CE(2)
CREF=CE(1)+CE(2)+CE(3)+CE(4)

C
C
C
CYCLE TIME FROM 0 TO 1/30 SECONDS IN 256 STEPS

DO 20 INC = 1,256
  T = DFLOAT(INC-1)/(256.D0*30.D0)
  CALCULATE RECEIVED FIELD FOR GIVEN TIME AND POSITION
  CREC=CREC+CP1*DSIN(OMEGAM*T)+CP2*DCOS(OMEGAM*T)
  XVR(INC) = DREAL(CREC)
  XVI(INC) = DIMAG(CREC)
20 CONTINUE

C
C
C
CALL FAST FOURIER TRANSFORM ROUTINE

CALL DPFFT(XVR,XVI,B)

C
C
C
LOOK AT THE 30 HERTZ COMPONENT AND DETERMINE THE PHASE

NI = 2
VARD = DATAN2(XVI(NI),XVR(NI))*(180.D0/PI)
IF(VARD.LT.0.0D0) VARD=VARD+360.D0
IF(VARD.GT.360.D0) VARD=VARD-360.D0

C
C
C
OBTAIN THE PHASE OF THE REFERENCE SIGNAL

REFD=DATAN2(DIMAG(CREF),DREAL(CREF))*180.D0/PI
IF(REFD.GT.360.D0) REFD=REFD-360.D0
IF(REFD.LT.0.0D0) REFD=REFD+360.D0

C
C
C
COMBINE ROTATING CARDIOD (VARD) AND ISOTROPIC REFERENCE SIGNAL,
AND ACCOUNT FOR INITIAL PHASING OF TONE WHEEL & GONIOMETER

VORAZD=(VARD+135.D0)-(REFD+90.D0)
IF(VORAZD.GT.360.D0) VORAZD=VORAZD-360.D0
IF(VORAZD.LT.0.0D0) VORAZD=VORAZD+360.D0

C
C
C
CALCULATE ERROR BETWEEN AZIMUTH ANGLE AND RECEIVED PHASE

ERROR = VORAZD - AZ
IF(ERROR.LT.-180.D0) ERROR=ERROR+360.D0
IF(ERROR.GT.180.D0) ERROR=ERROR-360.D0
PRINT 2, AZ,VORAZD,ERROR
2
  FORMAT(1X,3F15.5)
  WRITE(3,919)AZ,ERROR
919
  FORMAT(2F15.5)
30 CONTINUE
STOP
END

```

```

CCCCCCCCCCCCCCCCCCCCCCCCCCCCCCCCCCCCCCCCCCCCCCCCCCCCCCCCCCCCCCCC
C
C   THIS SUBROUTINE PROVIDES AN INTERFACE BETWEEN THE VOR MODEL 'GVOR'
C   AND THE 'NUMERICAL ELECTROMAGNETIC CODE'.
C
C   *****
C   SUBROUTINE NTG(PHI,VLTSPM,FAZ)
C   *****
C
CCCCCCCCCCCCCCCCCCCCCCCCCCCCCCCCCCCCCCCCCCCCCCCCCCCCCCCCCCCCCCCC
C   IMPLICIT REAL*8 (A,B,D-H,O-Z)
C   IMPLICIT COMPLEX*16 (C)
C   REAL*8 PHI,VLTSPM,FAZ
C   CHARACTER*12 POLARIZATION,TEST1
C   DIMENSION PHI(73,4),VLTSPM(73,4),FAZ(73,4)
C   DATA POLARIZATION/'POLARIZATION'/
C   PI=DACOS(-1.00)
CCCCCCCCCCCCCCCCCCCCCCCCCCCCCCCCCCCCCCCCCCCCCCCCCCCCCCCCCCCCCCCC
C   DO ONCE FOR EACH ANTENNA
C
C       DO 66 N=1,4
C
CCCCCCCCCCCCCCCCCCCCCCCCCCCCCCCCCCCCCCCCCCCCCCCCCCCCCCCCCCCCCCCC
C   READS COMPLEX CURRENTS FOR GVOR
C       DO 100 I=1,3000
C           READ(4,2,END=77) TEST1
C           FORMAT(55X,A12)
C           IF(POLARIZATION.EQ.TEST1) GOTO 333
100      CONTINUE
C
C       333      READ(4,44)
C       44      FORMAT(/)
C
C           DO 8 J=1,73
C               READ(4,5,END=77) PHI(J,N),VLTSPM(J,N),FAZ(J,N)
C               FORMAT(10X,F7.2,82X,E12.5,2X,F7.2)
C           5      CONTINUE
CCCCCCCCCCCCCCCCCCCCCCCCCCCCCCCCCCCCCCCCCCCCCCCCCCCCCCCCCCCCCCCC
C   SECTION TO CHECK OUTPUT
C       WRITE(6,7)N
C       7      FORMAT(1X,'N =',I3)
C           DO 9 J=1,73
C               WRITE(6,6) J,PHI(J,N),VLTSPM(J,N),FAZ(J,N)
C               6      FORMAT(3X,I2,3X,F7.2,3X,E11.5,3X,F7.2)
C           9      CONTINUE
CCCCCCCCCCCCCCCCCCCCCCCCCCCCCCCCCCCCCCCCCCCCCCCCCCCCCCCCCCCCCCCC
C
C       66      CONTINUE
C           RETURN

```





## NECIN.DAT

(NEC-2 input file for modeling a baseline VOR -- no scatterers)

Paul R. Barré

1 JUNE 1986

## GVOR ANTENNA MODEL

CM  
 CM  
 CM EACH STRUCTURE (1,2,3,4) IS A SQUARE ANTENNA WITH ALL OF IT'S SEGMENTS  
 CM BEING VOLTAGE SOURCES. EACH ANTENNA HAS A CIRCULAR RADIATION PATTERN  
 CM (ALFORD LOOP). THE COMBINED ANTENNAS FORM A VOR ANTENNA ARRAY.

CM

CM

CM

CM

CM

CM

CM

CM

CM

CM

CM

CM

CM

CM

CE

GW 1 1 -0.100 -0.100 0.0 -0.100 0.100 0.0 .0005

GW 2 1 -0.100 0.100 0.0 0.100 0.100 0.0 .0005

GW 3 1 0.100 0.100 0.0 0.100 -0.100 0.0 .0005

GW 4 1 0.100 -0.100 0.0 -0.100 -0.100 0.0 .0005

GM 0 0 0. 0. 0. .14500 .14500 1.2192 1.0

GE

GN 1

FR 0 0 0 0 110.2

EX 0 1 1 0 20000.0

EX 0 2 1 0 20000.0

EX 0 3 1 0 20000.0

EX 0 4 1 0 20000.0

RP 0 1 73 1500 85.77 0. 0. 5. 18525.

NX

CM ANTENNA TWO RUN

CE

GW 1 1 -0.100 -0.100 0.0 -0.100 0.100 0.0 .0005

GW 2 1 -0.100 0.100 0.0 0.100 0.100 0.0 .0005

GW 3 1 0.100 0.100 0.0 0.100 -0.100 0.0 .0005

GW 4 1 0.100 -0.100 0.0 -0.100 -0.100 0.0 .0005

GM 0 0 0. 0. 0. .14500 -.14500 1.2192 1.0

GE

GN 1

FR 0 0 0 0 110.2

EX 0 1 1 0 20000.0

EX 0 2 1 0 20000.0  
EX 0 3 1 0 20000.0  
EX 0 4 1 0 20000.0  
RP 0 1 73 1500 85.77 0. 0. 5. 18525.  
NX

CM ANTENNA THREE RUN

CE  
GW 1 1 -0.100 -0.100 0.0 -0.100 0.100 0.0 .0005  
GW 2 1 -0.100 0.100 0.0 0.100 0.100 0.0 .0005  
GW 3 1 0.100 0.100 0.0 0.100 -0.100 0.0 .0005  
GW 4 1 0.100 -0.100 0.0 -0.100 -0.100 0.0 .0005  
GM 0 0 0. 0. 0. -.14500 .14500 1.2192 1.0

GE

GN 1

FR 0 0 0 0 110.2  
EX 0 1 1 0 20000.0  
EX 0 2 1 0 20000.0  
EX 0 3 1 0 20000.0  
EX 0 4 1 0 20000.0  
RP 0 1 73 1500 85.77 0. 0. 5. 18525.

NX

CM ANTENNA FOUR RUN

CE

GW 1 1 -0.100 -0.100 0.0 -0.100 0.100 0.0 .0005  
GW 2 1 -0.100 0.100 0.0 0.100 0.100 0.0 .0005  
GW 3 1 0.100 0.100 0.0 0.100 -0.100 0.0 .0005  
GW 4 1 0.100 -0.100 0.0 -0.100 -0.100 0.0 .0005  
GM 0 0 0. 0. 0. -.14500 -.14500 1.2192 1.0

GE

GN 1

FR 0 0 0 0 110.2  
EX 0 1 1 0 20000.0  
EX 0 2 1 0 20000.0  
EX 0 3 1 0 20000.0  
EX 0 4 1 0 20000.0  
RP 0 1 73 1500 85.77 0. 0. 5. 18525.

EN



GW 1 1 -0.100 -0.100 0.0 -0.100 0.100 0.0 .0005  
 GW 2 1 -0.100 0.100 0.0 0.100 0.100 0.0 .0005  
 GW 3 1 0.100 0.100 0.0 0.100 -0.100 0.0 .0005  
 GW 4 1 0.100 -0.100 0.0 -0.100 -0.100 0.0 .0005  
 GM 0 0 0. 0. 0. .14500 -.14500 1.2192 1.0  
 GW 15 2 0. -0.0525 -0.21 0. 0.0525 -0.21 .00795  
 GW 16 6 0. -0.0525 -0.21 0. -0.0525 0.0 0.00795  
 GW 17 6 0. 0.0525 -0.21 0. 0.0525 0.0 0.00795  
 GW 18 3 0. -0.0525 0.0 0. -0.5125 0.0 0.00795  
 GW 19 3 0. 0.0525 0.0 0. 0.5125 0.0 0.00795  
 GM 0 0 0. -10.83 0. 1.310 0. 1.2192 15.0  
 GM 0 0 0. 0. 0.0 0. 0. 0. 15.0

GE

GN 1

FR 0 0 0 0 110.2  
 EX 0 1 1 0 20000.0  
 EX 0 2 1 0 20000.0  
 EX 0 3 1 0 20000.0  
 EX 0 4 1 0 20000.0  
 RP 0 1 73 1500 82.94 0. 0. 5. 11115.4

NX

CM ANTENNA THREE RUN

CE

GW 1 1 -0.100 -0.100 0.0 -0.100 0.100 0.0 .0005  
 GW 2 1 -0.100 0.100 0.0 0.100 0.100 0.0 .0005  
 GW 3 1 0.100 0.100 0.0 0.100 -0.100 0.0 .0005  
 GW 4 1 0.100 -0.100 0.0 -0.100 -0.100 0.0 .0005  
 GM 0 0 0. 0. 0. -.14500 .14500 1.2192 1.0  
 GW 15 2 0. -0.0525 -0.21 0. 0.0525 -0.21 .00795  
 GW 16 6 0. -0.0525 -0.21 0. -0.0525 0.0 0.00795  
 GW 17 6 0. 0.0525 -0.21 0. 0.0525 0.0 0.00795  
 GW 18 3 0. -0.0525 0.0 0. -0.5125 0.0 0.00795  
 GW 19 3 0. 0.0525 0.0 0. 0.5125 0.0 0.00795  
 GM 0 0 0. -10.83 0. 1.310 0. 1.2192 15.0  
 GM 0 0 0. 0. 0.0 0. 0. 0. 15.0

GE

GN 1

FR 0 0 0 0 110.2  
 EX 0 1 1 0 20000.0  
 EX 0 2 1 0 20000.0  
 EX 0 3 1 0 20000.0  
 EX 0 4 1 0 20000.0  
 RP 0 1 73 1500 82.94 0. 0. 5. 11115.4

NX

CM ANTENNA FOUR RUN

CE

GW 1 1 -0.100 -0.100 0.0 -0.100 0.100 0.0 .0005  
 GW 2 1 -0.100 0.100 0.0 0.100 0.100 0.0 .0005  
 GW 3 1 0.100 0.100 0.0 0.100 -0.100 0.0 .0005  
 GW 4 1 0.100 -0.100 0.0 -0.100 -0.100 0.0 .0005  
 GM 0 0 0. 0. 0. -.14500 -.14500 1.2192 1.0

GW 15 2 0. -0.0525 -0.21 0. 0.0525 -0.21 .00795  
GW 16 6 0. -0.0525 -0.21 0. -0.0525 0.0 0.00795  
GW 17 6 0. 0.0525 -0.21 0. 0.0525 0.0 0.00795  
GW 18 3 0. -0.0525 0.0 0. -0.5125 0.0 0.00795  
GW 19 3 0. 0.0525 0.0 0. 0.5125 0.0 0.00795  
GM 0 0 0. -10.83 0. 1.310 0. 1.2192 15.0  
GM 0 0 0. 0. 0.0 0. 0. 0. 15.0  
GE  
EN 1  
FR 0 0 0 0 110.2  
EX 0 1 1 0 20000.0  
EX 0 2 1 0 20000.0  
EX 0 3 1 0 20000.0  
EX 0 4 1 0 20000.0  
RP 0 1 73 1500 82.94 0. 0. 5. 11115.4  
EN

APPENDIX C

USER'S SECTION

General guidelines for NEC-2 wire modeling are presented in this section. Also, an example is given that illustrates how to add a scatterer to the baseline VOR model input file, NECIN.DAT, with the intention of introducing the reader to the NEC-2 "punched card" format. This section is not meant to provide a working knowledge of NEC-2, but only to give a general description of the user interface. The more interested reader is referred to the NEC-2 User's Guide [1]. The complete listing for NECIN.DAT may be found in Appendix B.

Proper choice of the wire segments for a model is the most critical step in obtaining accurate results. Wire segments are defined by the coordinates of their two end points and their radius. Both geometrical and electrical factors must be considered when modeling a structure with wire segments.

Geometrically, the segments should follow the conductor paths as closely as possible, using a piece-wise linear approach on curves. Also, wires should be connected together only by joining segment ends. Although segments are treated as connected if the separation of their ends is less than about  $10^{-3}$  times the length of the shortest segment, the segment ends of two joining wires should have identical space coordinates when possible. The angle of intersection for wire segments is not restricted in any manner.

Electrically, a wire may be given any radius "a" as long as  $6\pi a$  divided by the exciting wavelength is much less than one. Furthermore, a wire may need to be divided into segments to satisfy the electrical

requirements of segment length relative to wavelength. The number of segments that a wire can be divided into is up to the user. However, as a general guide for accuracy, wire segments should be less than 0.1 times the exciting wavelength and greater than 0.05 times this wavelength. There are certain conditions under which these limits may be extended: somewhat longer segments may be acceptable for long wires with no abrupt changes, whereas shorter segments may be necessary for modeling critical areas of an antenna.

In NEC-2 a wire is constructed (input to the program) in the following manner:

1. The wire is first given a tag number. The number of segments that this wire is divided into is also specified. A particular wire segment can be uniquely identified by its tag and segment number, sort of like a first and last name.
2. The location of the wire with respect to the origin of a rectangular coordinate system is then given by two pairs of XYZ coordinates. Which end of the wire is specified as end one does not matter unless the wire is to be excited by a voltage source. In this case, end one takes on negative polarity while end two becomes the positive side, causing current to flow from point one to point two.
3. The wire radius is then specified. If a wire radius is needed that is larger than the limit specified above, then NEC-2 can be asked to perform all calculations on that wire using an extended thin



wire kernel. With the extended thin wire kernel, a wire is modeled as a tube rather than as a filament. [Special treatment must be given if the wire to be modeled in this manner has a bend in it, because the current will not be continuous around the circumference of the tube at the bend.]

Data to describe an antenna and its environment and to request computation of antenna characteristics are input by means of a "punched card", one line at a time, format. The data card deck for a single run of NEC-2 consists of three types of data cards: (1) COMMENTS: The deck begins with one or more comment cards (CM), followed by the CE card which stands for "Comments End". Lines 1 and 2 of the NECIN.DAT excerpt shown below form the comment section for Antenna One Run. (2) GEOMETRY: Geometry data cards specify the geometry of the antennas and scatterers. Lines 3 through 7 specify antenna #1 to the program, and line eight, the GE card, ends the Geometry section. (3) CONTROL: The deck ends with a section of program control cards specifying electrical parameters such as frequency, loading and excitation, and requests for calculation of antenna currents and fields. Lines 9 through 15 below specify a ground plane, the frequency, the excitations, and the request for radiation patterns for the first of four program runs.

Example: Add a scatterer to the NECIN.DAT excerpt given below, Antenna-One-Run, that has the same dimensions as the transmitting antenna, but is located symmetrically on the other side of the X axis. The X and Z

coordinates remain the same. Note that the transmitting antenna is defined by lines 3 through 6, and positioned by line 7.

## NECIN.DAT

	Column Numbers											
	1	2	3	4	5	6	7	8	9	10	11	12
Card #	1	2	3	4	5	6	7	8	9	10	11	12
	CM		ANTENNA	ONE	RUN							
	2	CE										
	3	GW	1	2	-0.100	-0.100	0.0	-0.100	0.100	0.0	.0005	
	4	GW	2	1	-0.100	0.100	0.0	0.100	0.100	0.0	.0005	
	5	GW	3	1	0.100	0.100	0.0	0.100	-0.100	0.0	.0005	
	6	GW	4	1	0.100	-0.100	0.0	-0.100	-0.100	0.0	.0005	
	7	GM	0	0	0.	0.	0.	.14500	.14500	1.2192	1.0	
	8	GE										
	9	GN	1									
	10	FR	0	0	0	0	110.2					
	11	EX	0	1	1	0	20000.0					
	12	EX	0	2	1	0	20000.0					
	13	EX	0	3	1	0	20000.0					
	14	EX	0	4	1	0	20000.0					
	15	RP	0	1	73	1500	85.77	0.	0.	5.	18525.	
	16	NX										
	17	CM		ANTENNA	TWO	RUN	...	etc.				

Solution: The coordinate transformation card (GM) is used to form a duplicate of the transmitting antenna and locate it in the desired position. This full ability of this card is to translate or rotate a structure with respect to the coordinate system, or to generate new duplicate structures translated or rotated from the original. The card has the following format:

```
GM ITG1 NRPT ROX ROY ROZ XS YS ZS ITS
```

where ITG1 is the tag number increment, NRPT is the number of new structures to be generated, ROX-r-Z specify rotation, X-Y-ZS specify translation, and ITS is the tag number at which to begin duplication (a process that continues up to the specifying GM card).

The tag numbers for the four GW cards (that define the antenna) run from 1 to 4. So that the next tag number is in sequence (5), ITG1 is set to 4 + 4 = 5). Only one new structure is to be generated, so NRPT is set to 1. All rotation parameters are set to 0. For the translation parameters, YS is set to  $-(2 * 0.14500)$ , and the other two are set to zero. The card is placed in the file between lines 7 and 8, and has the following appearance:

```
GM 4 1 0. 0. 0. 0. -0.290 0. 1.
```

It should be noted that the NEC-2 user interface assumes an understanding of the theory and solution method employed. The user encountering the code for the first time should begin with the User's Guide and try to model some simple antennas. The understanding gained will assist in the proper preparation of input and the proper interpretation of output.

## VIII. ABSTRACT

Barré, Paul Reldon. June, 1986 Electrical Engineering

*Implementation of the Numerical Electromagnetic Code (NEC-2) for Modeling the VOR Navigation System in the Presence of Parasitic Scatterers.* (107pp.)

A computer model has been developed that estimates bearing error for a VOR airborne navigation system operating in the presence of small, parasitic scatterers such as antennas, antenna masts, and guy wires. This model, which is written using FORTRAN 77, interacts with an unmodified version of the Numerical Electromagnetics Code (NEC-2) to obtain the pertinent scattered-field data. These data are then used to calculate the composite field, and indicated bearing, at the airborne receiver location. Modeled results consist of plots of bearing error versus "true" bearing. Comparisons of modeled and measured data are presented.

The azimuth angle of an aircraft with respect to a VOR station is determined by the phase of the received audio sinusoid generated by a limacon radiation pattern that rotates in space due to appropriate time-varying phasing between four Alford loop antennas. To model the effects of scatterers on system accuracy, each loop antenna is sequentially modeled in the presence of the scatterer using NEC-2, and field data are recorded for a far-field orbit around the source-scatterer configuration; this process is repeated for each of the four loop antennas thus providing complete information about complex path loss between each loop antenna and the observation point in the presence of

the scatterer. The received audio waveform is then constructed at each observation point by applying the appropriate modulation to each of the loop antennas, adjusted by the complex loss values given by NEC-2. The phase and distortion of the received audio waveform is determined using a Fast Fourier Transform algorithm.

The key points addressed include approximations for modeling the Alford Loop antennas (which involves attempts at surface patch excitation), representation of the ground plane, model diagnostics, and comparisons of modeled and measured data. A user section is also included to give guidance in the modeling of parasitic scatterers.